Finite-Volume Methods in Meteorology
- a semi-Lagrangian view

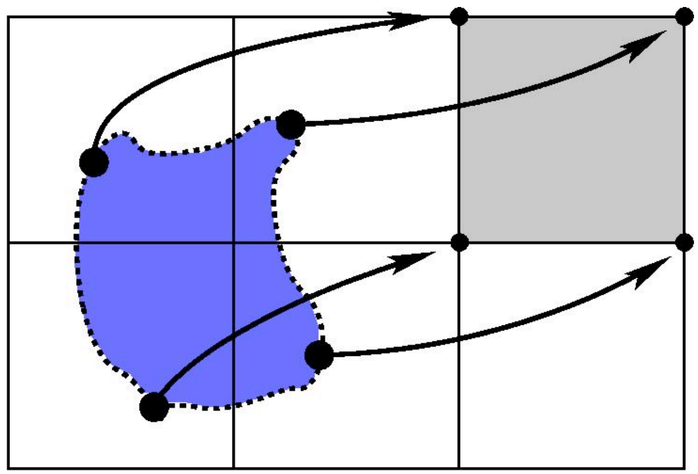

Peter Hjort Lauritzen

Atmospheric Modeling & Predictability Section

National Center for Atmospheric Research

- This talk is heavily biased towards a Lagrangian way of thinking
- The review is non-exhaustive and many schemes are not discussed; see, e.g., extensive reviews in the computational fluid dynamics (CFD) literature such as LeVeque (2002) and Eymard et al. (2000).

Outline

- Introduction
- Desirable properties for transport schemes intended for atmospheric flow problems
- Eulerian versus Lagrangian discretizations (and the equivalence between the two)
- Sub-grid-cell reconstruction
- Lagrangian finite-volume transport schemes
- Eulerian finite-volume transport schemes

"Simplifying Assumptions"

- For simplicity I will explain methods on squared meshes in Cartesian geometry although most methods could be (in principle), or have been, generalized to other meshes (some with less, some with more ease) .
- Almost all schemes I will discuss have been extended to spherical geometry.

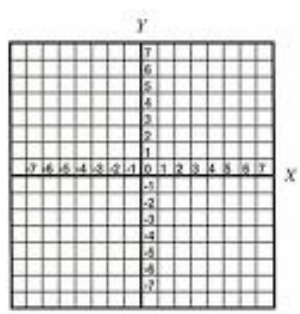

square mesh

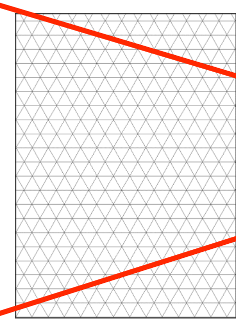

triangles

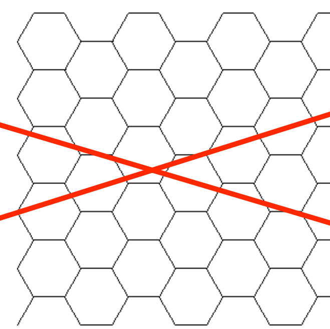

hexagons

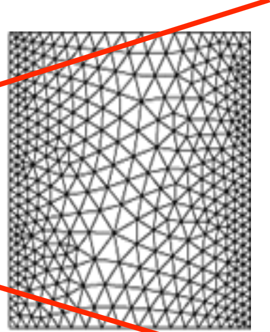

unstructured

Definition

Finite-volume methods are numerical methods, where the fundamental prognostic variable considered is an integrated quantity over a certain finite-control volume.

Also referred to as *cell-integrated methods*.

Definition

Finite-volume methods are numerical methods, where the fundamental prognostic variable considered is an integrated quantity over a certain finite-control volume.

Also referred to as *cell-integrated methods*.

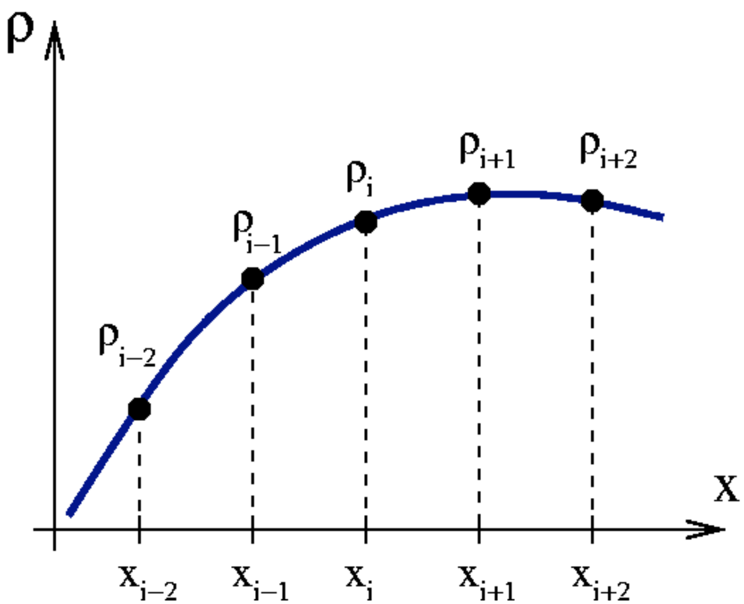

Thus, instead of representing the solution in terms of grid-point values (used in, e.g., finite-difference methods),

$$\rho = \rho_i = \rho(x_i)$$

Definition

Finite-volume methods are numerical methods, where the fundamental prognostic variable considered is an integrated quantity over a certain finite-control volume.

Also referred to as *cell-integrated methods*.

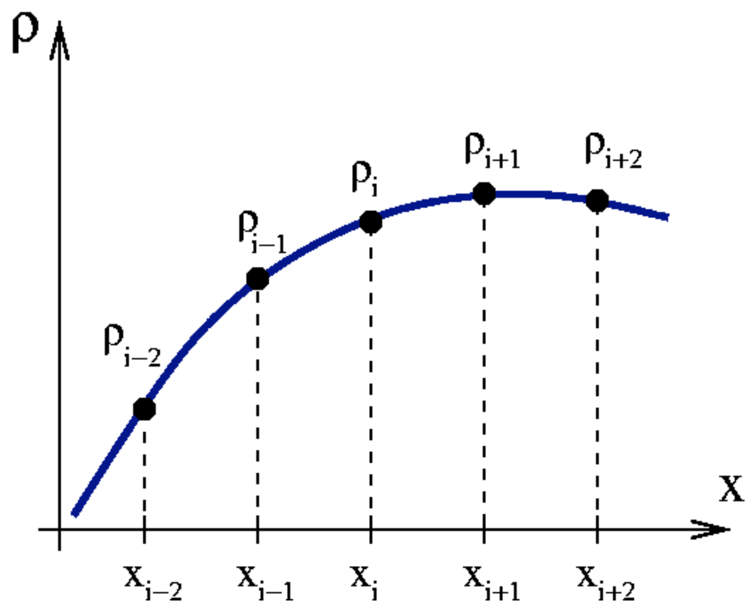

Thus, instead of representing the solution in terms of grid-point values (used in, e.g., finite-difference methods), weights for expansion functions (finite-element methods, e.g., spectral method),

Definition

Finite-volume methods are numerical methods, where the fundamental prognostic variable considered is an integrated quantity over a certain finite-control volume.

Also referred to as *cell-integrated methods*.

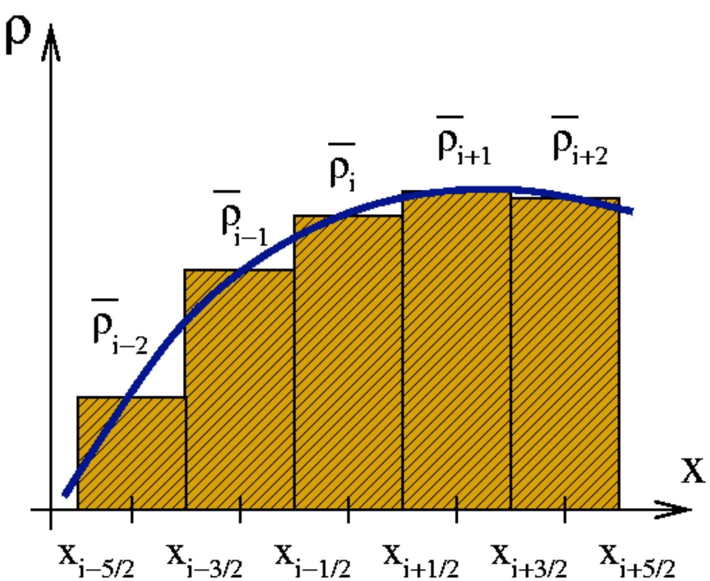

Thus, instead of representing the solution in terms of grid-point values (used in, e.g., finite-difference methods), weights for expansion functions (finite-element methods, e.g., spectral method), *cell-integrated mean values* are considered.

Definition

Finite-volume methods are numerical methods, where the fundamental prognostic variable considered is an integrated quantity over a certain finite-control volume.

Also referred to as *cell-integrated methods*.

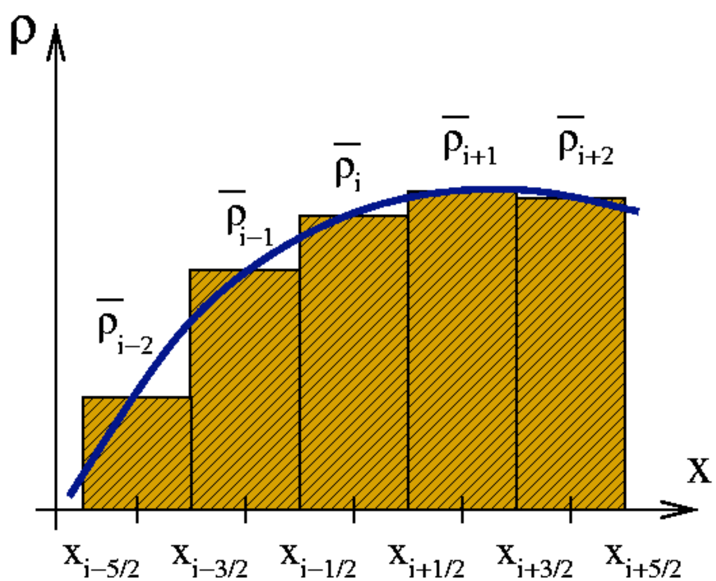

Finite-volume schemes are inherently conservative with respect to the prognostic variable.

Focus on finite-volume methods for the continuity equation for tracers
(transport equation)

- Before discussing the different finite-volume schemes used in the atmospheric sciences, it is important to realize which properties a transport scheme ideally should possess: Desirable properties!
- The equation subject to the toughest requirements is probably the continuity equation for tracers, such as moisture, for which the spatial distribution includes sharp gradients.

Desirable properties

- Accuracy: Formal truncation error

For sufficiently smooth problems accuracy can be assessed with Taylor Series, e.g.:

Consider one-dimensional advection equation (constant v) $$\frac{\partial \rho}{\partial t} + v\frac{\partial \rho}{\partial x} = 0$$

A simple finite-difference approximation ("upstream" or "donor-cell" scheme)

$$\frac{\rho_j^{n+1} - \rho_j^n}{\Delta t} + v\frac{\rho_j^n - \rho_{j-1}^n}{\Delta x} = 0$$

Insert Taylor series expansion about $(n\Delta t, j\Delta x)$ to get truncation error:

$$\frac{\rho_j^{n+1} - \rho_j^n}{\Delta t} + v\frac{\rho_j^n - \rho_{j-1}^n}{\Delta x} = \frac{\Delta t}{2}\frac{\partial^2 \rho}{\delta t^2} - v\frac{\Delta x}{2}\frac{\partial^2 \rho}{\delta x^2} + ...$$

The "upstream" scheme is first-order accurate in space and time.

Desirable properties

- Accuracy: Formal truncation error

However, for flows with shocks or sharp gradients the formal order of accuracy in terms of a Taylor series expansions does not necessarily guarantee a high level of accuracy, e.g., advection of a square wave:

second-order scheme (Crank-Nicolson)

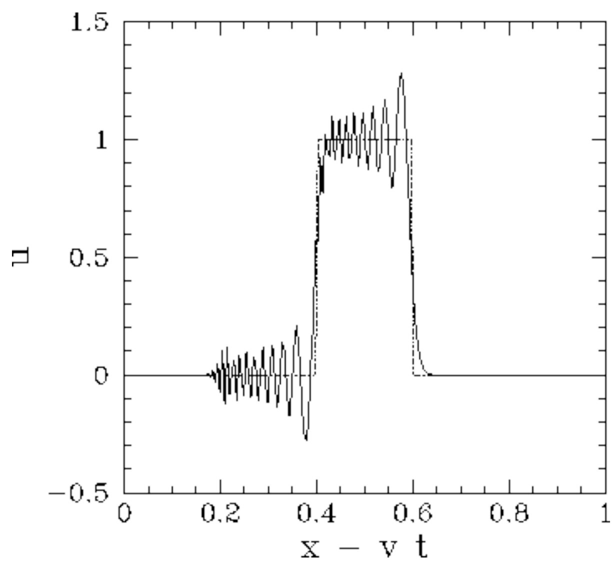

first-order scheme ("upwind")

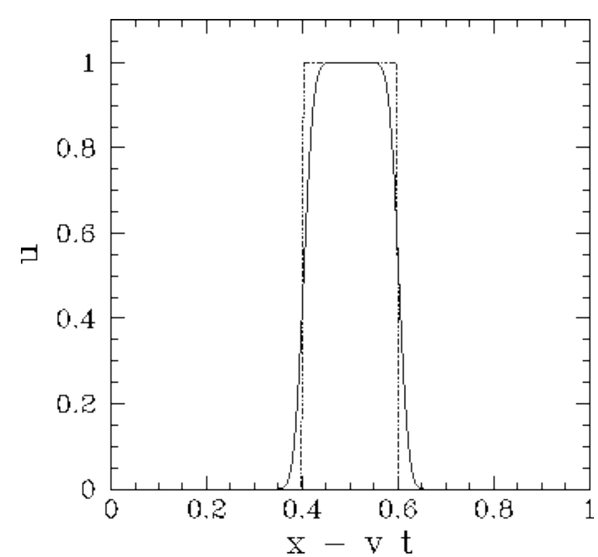

Desirable properties

- Accuracy: Stability analysis

The linear dissipation and dispersion properties can be assessed by a **Von Neumann stability analysis** by representing the discretized solution by a finite Fourier series of the form

$$\rho_j^n = \sum_{k=-N}^{N} a_k^n e^{ikj\Delta x}$$

and examine the stability of the individual Fourier components.

Purely dissipative numerical scheme

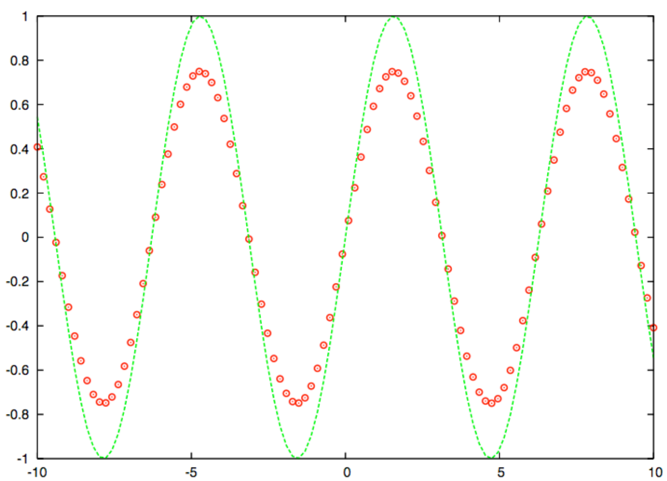

Purely dispersive numerical scheme

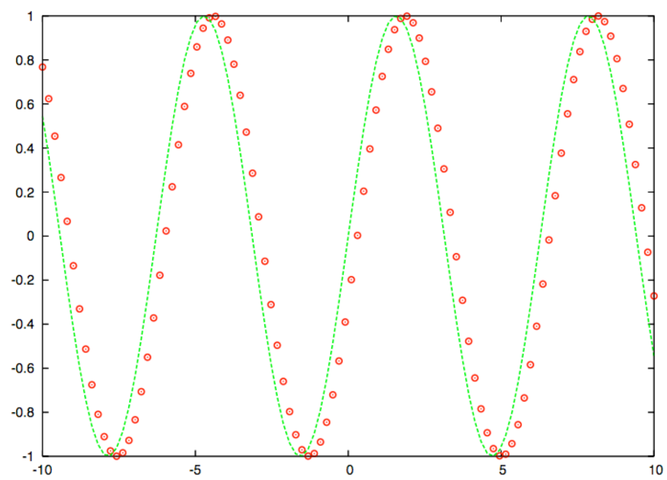

Desirable properties

- Accuracy: Stability analysis

A **Von Neumann stability analysis** is **linear**: We assume constant velocities/coefficients and turn off any non-linearity in the numerical scheme such as filters.

E.g. a Von Neumann analysis of the Lin & Rood advection scheme with second-order inner operators and third-order outer operators for a constant traverse flow shows that the scheme is slightly unstable BUT when turning on a filter then the scheme becomes diffusive and stable.

Maximum value of numerical solution for sine wave advection

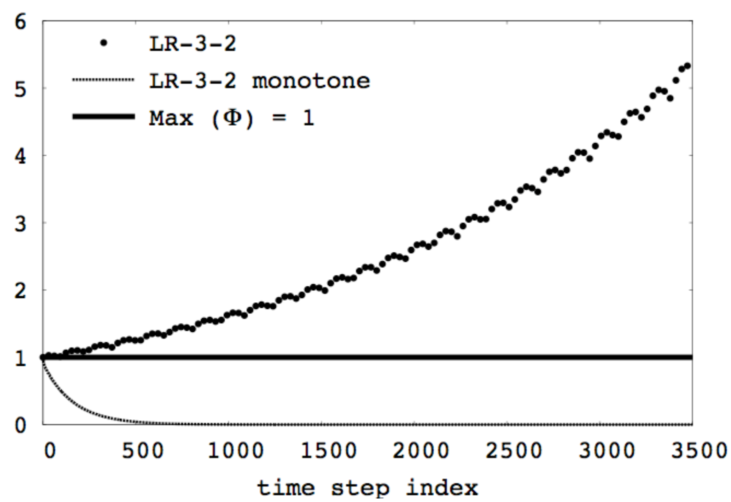

Lauritzen (MWR, 2007)

Desirable properties

- Accuracy: Idealized test cases

Idealized tests, where the analytical solution is known, are widely used to assess the accuracy of transport schemes. The accuracy is usually assessed in terms of standard error measures (RMS, etc.).

Examples of idealized passive tracer advection tests:

Translational tests

Probably the most commonly used idealized test case in the meteorological literature is the solid body rotation of a cosine cone or slotted cylinder (in Cartesian and spherical geometry).

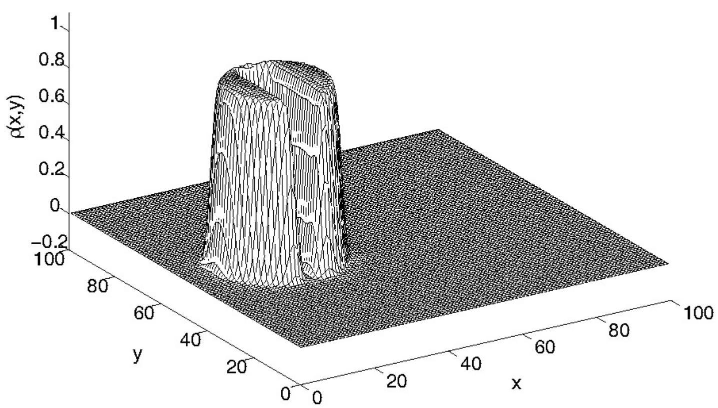

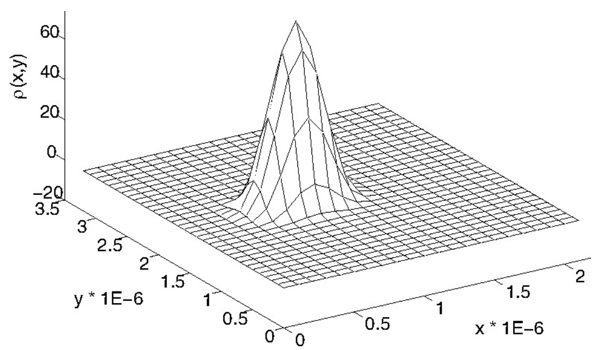

Zalesak (1979), Bermejo and Staniforth (1992), Williamson et al. (1992)

Desirable properties

- Accuracy: Idealized test cases

Idealized tests, where the analytical solution is known, are widely used to assess the accuracy of transport schemes. The accuracy is usually assessed in terms of standard error measures (RMS, etc.).

Examples of idealized passive tracer advection tests:

Deformational tests

- swirling shear flow specified in terms of a periodically reversing time-dependent velocity field (Durran, 1999).
- deformational flow test where the solution is known throughout the time of integration (Smolarkiewicz (1982), Staniforth et al. (1987))
- Idealized cyclogenesis (Doswell (1984), Rancic (1992), Holm (1995), Nair et al. (1999)).

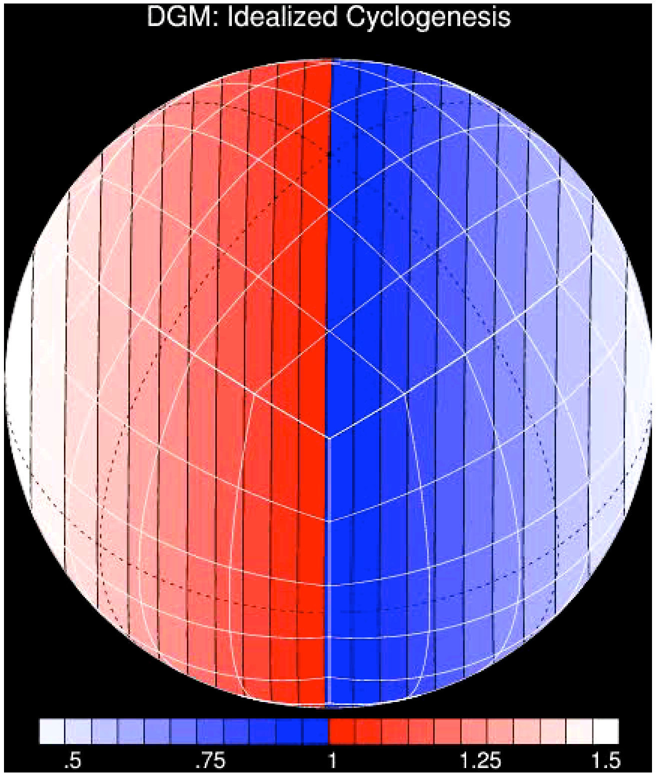

Movie courtesy of Ram Nair

Desirable properties

- Accuracy: Idealized test cases

Idealized tests, where the analytical solution is known, are widely used to assess the accuracy of transport schemes. The accuracy is usually assessed in terms of standard error measures (RMS, etc.).

Examples of idealized passive tracer advection tests:

Combination of translational and deformational test

• Moving vortex (Nair and Jablonowski, 2008).

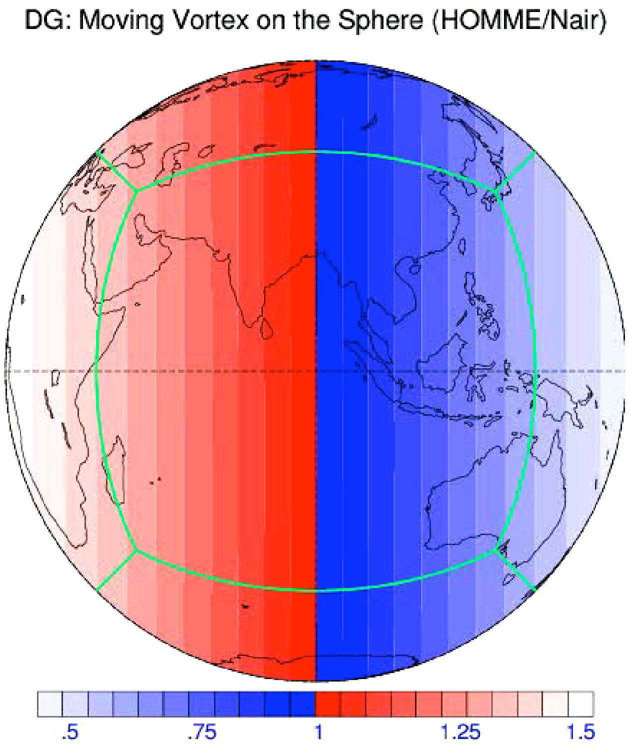

Movie courtesy of Ram Nair

Desirable properties

- Accuracy: Idealized test cases

Idealized tests where the analytical solution is known are widely used to assess the accuracy of transport schemes. The accuracy is usually assessed in terms of standard error measures (RMS, etc.).

Note, however, that good performance in idealized settings does not necessarily imply that the scheme will work well in a “full” model with “real” data!

But if a scheme does not do well in idealized test cases it is likely that it will not do well in a “full” model.

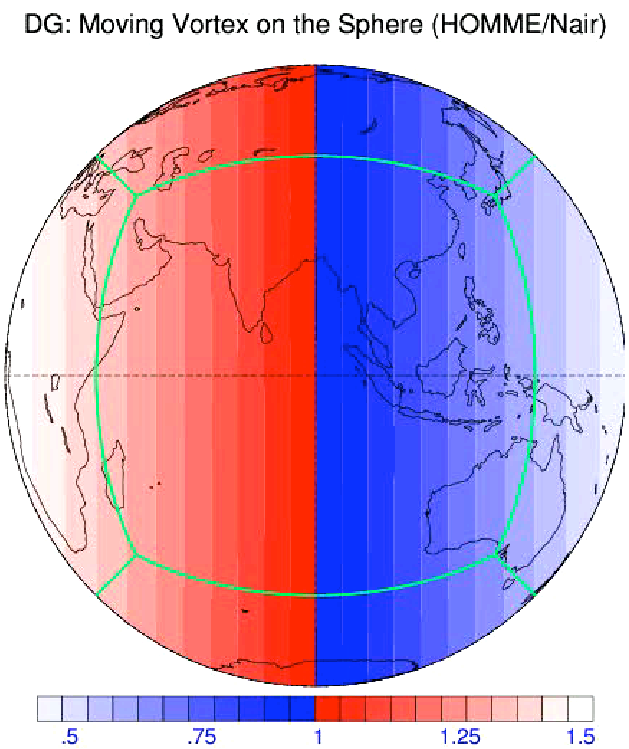

Movie courtesy of Ram Nair

Desirable properties

- Accuracy
- Computational efficiency: accuracy versus cost

Should we use a computationally cheap scheme (on a given platform) that is less accurate that we can afford to run at higher resolution, or should we use an expensive scheme that is more accurate but that we can only afford to run at coarser resolution?

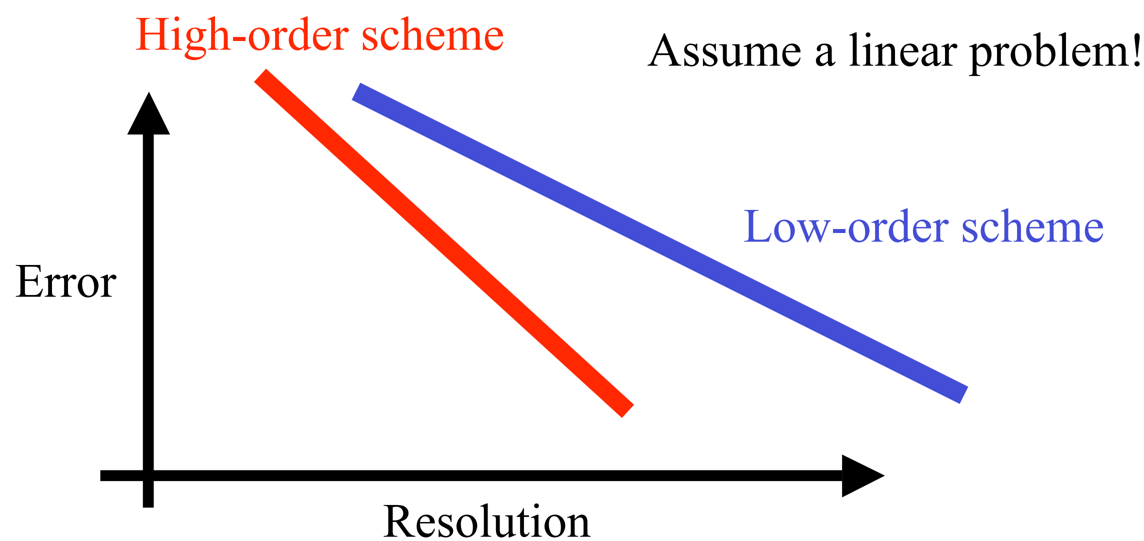

Desirable properties

- Accuracy
- Computational efficiency: accuracy versus cost

Should we use a computationally cheap scheme (on a given platform) that is less accurate that we can afford to run at higher resolution, or should we use an expensive scheme that is more accurate but that we can only afford to run at coarser resolution?

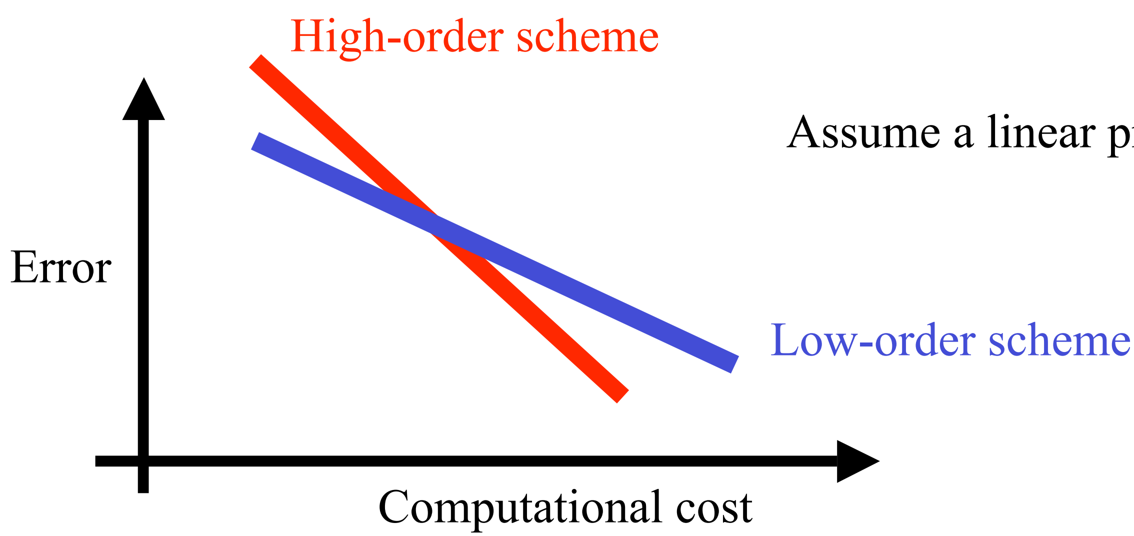

Assume a linear problem!

Desirable properties

- Accuracy
- Computational efficiency: accuracy versus cost
- Shape-preservation, positive-definiteness, monotonicity, non-oscillatory

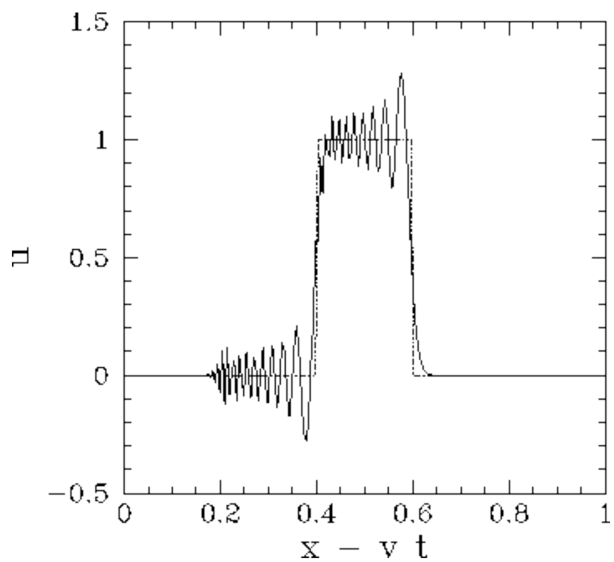

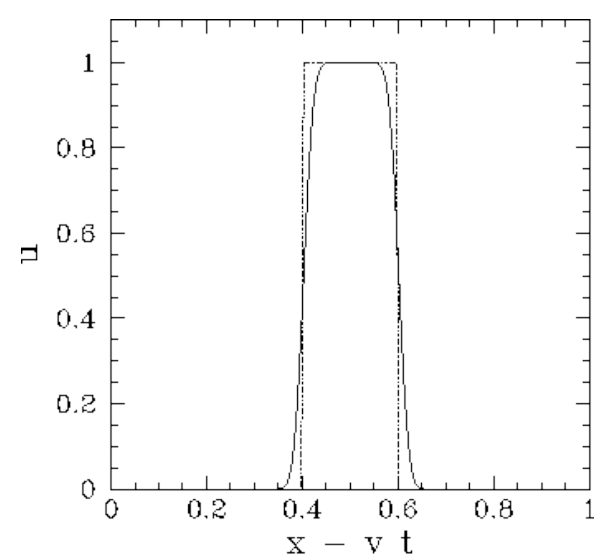

Desirable properties

- Accuracy
- Computational efficiency: accuracy versus cost
- Shape-preservation, positive-definiteness, monotonicity, non-oscillatory
- Conservation
- Locality
- Preservation of constancy in a non-divergent flow field
- See Machenhauer et al. (2008) for a longer list

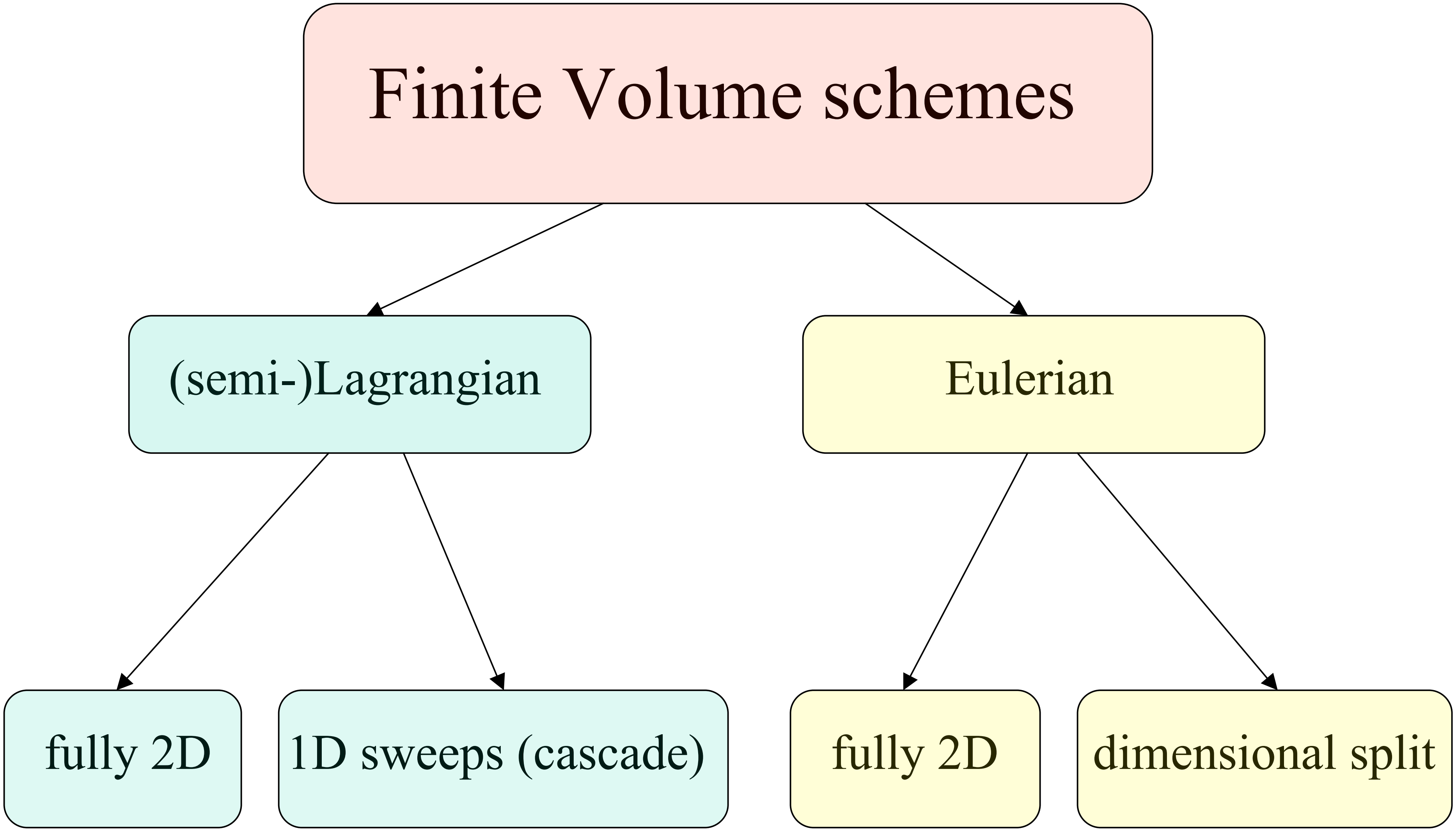
Finite Volume schemes
(semi-)Lagrangian
Eulerian
fully 2D
1D sweeps (cascade)
fully 2D
dimensional split

Eulerian versus Lagrangian

Equations of motion for the atmosphere can be derived from first principles in either a *Lagrangian* or an *Eulerian* form:

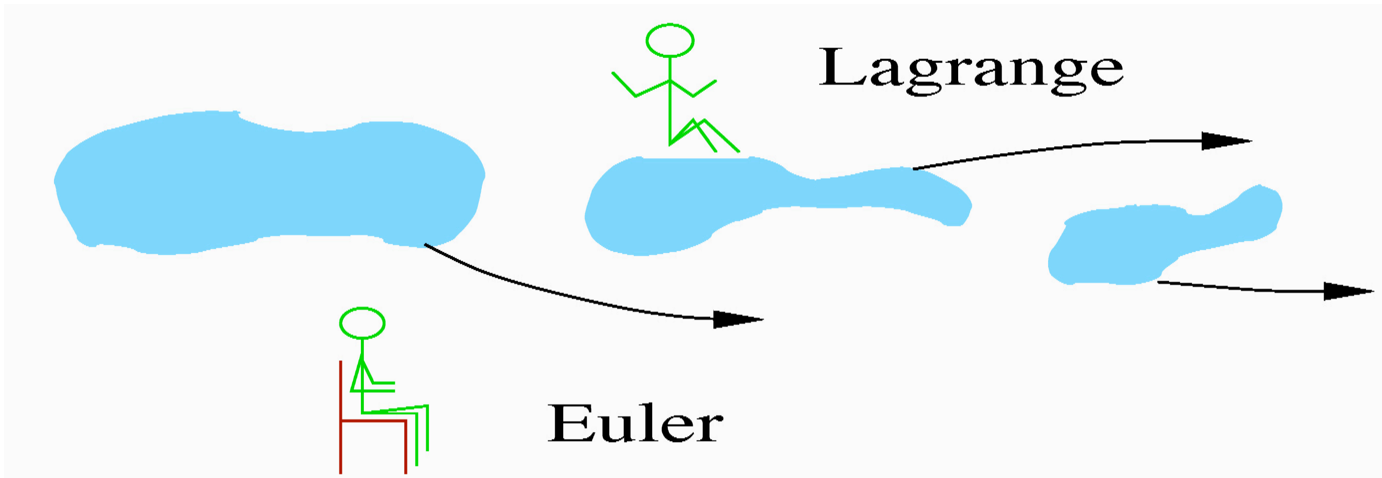

From Prof. Thuburn's talk

Lagrangian
Describe evolution of the flow as would be observed following the motion of an individual fluid parcel

Eulerian
Describe evolution of the flow from a fixed point in a coordinate system rotating with the Earth

Continuity equation: Eulerian and Lagrangian form

Consider the two-dimensional mass continuity equation for a passive tracer ρ (no sources/ sinks) in Eulerian flux form:

$$\boxed{\frac{\partial \rho}{\partial t} + \nabla \cdot (\vec{v}\rho) = 0}$$

where $\vec{v}$ is the velocity vector and ρ is the density of the tracer. The Lagrangian form of the continuity equation is obtained through the following operations:

$$\frac{\partial \rho}{\partial t} + \vec{v}\nabla\rho = -\rho\nabla\cdot\vec{v} \quad \Leftrightarrow \quad \frac{D\rho}{Dt} = -\rho\nabla\cdot\vec{v} \qquad \text{where} \quad \frac{D}{Dt} = \frac{\partial}{\partial t} + \vec{v}\nabla$$

The divergence $\nabla \cdot \vec{v}$ can also be written in Lagrangian form $\boxed{\left[\frac{1}{\delta A}\frac{D}{Dt}(\delta A)\right]}$ where δA is an infinitesimal area moving with the flow.

Substituting the Lagrangian divergence into the equation above and using the chain rule for differentiation yields the Lagrangian form of the continuity equation:

$$\boxed{\frac{D}{Dt}[\rho\,\delta A] = 0}$$

Note that the divergence does not appear explicitly

Cell-integrated semi-Lagrangian (CISL) scheme

Integrate Lagrangian continuity equation over a cell/volume *A* moving with the flow:

$$\frac{D}{Dt}\left[\iint_A \rho \, dx \, dy\right] = 0$$

Discretizing this equation using backward trajectories, the CISL continuity equation results:

$$\overline{\rho}^{n+1}\Delta A = \overline{\rho}_*^n \delta A$$

where ΔA and δA is referred to as the *departure* and *arrival* area, respectively.

$$\overline{\rho}_*^n = \frac{1}{\delta A}\iint_{\delta A} \rho^n(x,y) \, dx \, dy$$

is the is the integral of $\rho^n(x,y)$ over the departure area, where $\rho^n(x,y)$ is the sub-grid-scale reconstruction.

More on reconstructions later …

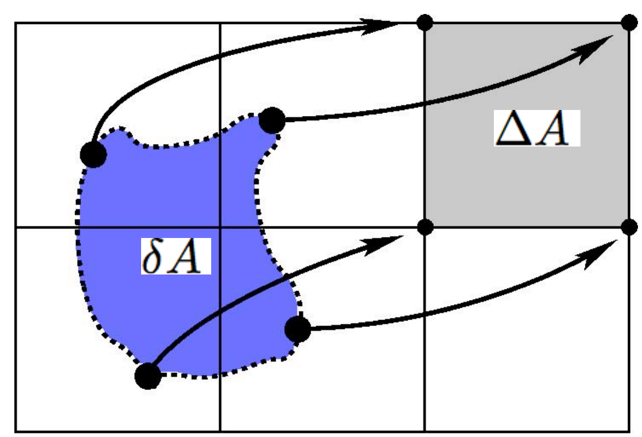

Cell-integrated semi-Lagrangian (CISL) scheme

Integrate Lagrangian continuity equation over a cell/volume A moving with the flow:

$$\frac{D}{Dt}\left[\iint_A \rho \, dx\, dy\right] = 0$$

Discretizing this equation using backward trajectories, the CISL continuity equation results:

$$\overline{\rho}^{n+1}\Delta A = \overline{\rho}_*^{n}\delta A$$

where ΔA and δA is referred to as the *departure* and *arrival* area, respectively.

Note: If the departure area (trajectories) is exact and the reconstruction and integral thereof over the departure area is exact then the discretized CISL equation is exact!

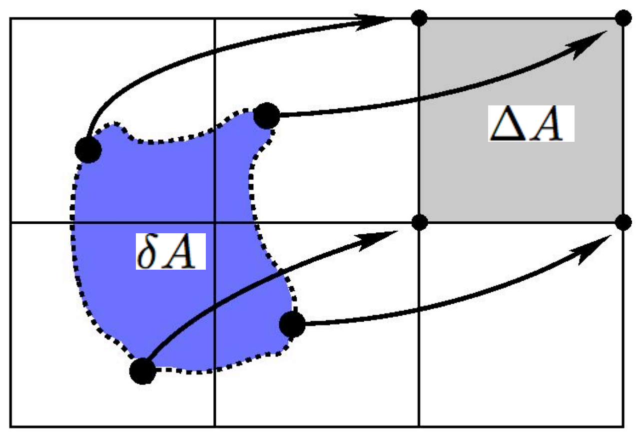

Eulerian finite-volume scheme

Integrate the flux-form Eulerian continuity equation

$$\boxed{\frac{\partial \rho}{\partial t} + \nabla \cdot (\vec{v}\rho) = 0}$$

over the arrival area ΔA an apply Gauss's divergence theorem:

$$\frac{\partial}{\partial t}\left[\iint_{\Delta A} \rho \, dx\, dy\right] = -\iint_{\Delta A} \nabla \cdot (\rho \vec{v}) \; dx\, dy = -\iint_{\partial(\Delta A)} \rho\, \vec{v} \cdot \vec{n}\, d\ell$$

where $\vec{n}$ is the outward pointing unit normal vector of the boundary $\partial(\Delta A)$. Discretizing the left-hand side and time-averaging the right-hand side, yields:

$$\overline{\rho}^{n+1}\Delta A = \overline{\rho}^{n}\Delta A - \Delta t \sum_{i=1}^{4}\left[\overline{\overline{\langle \rho \vec{v} \rangle}} \cdot \vec{n}\, \Delta \ell\right]_i$$

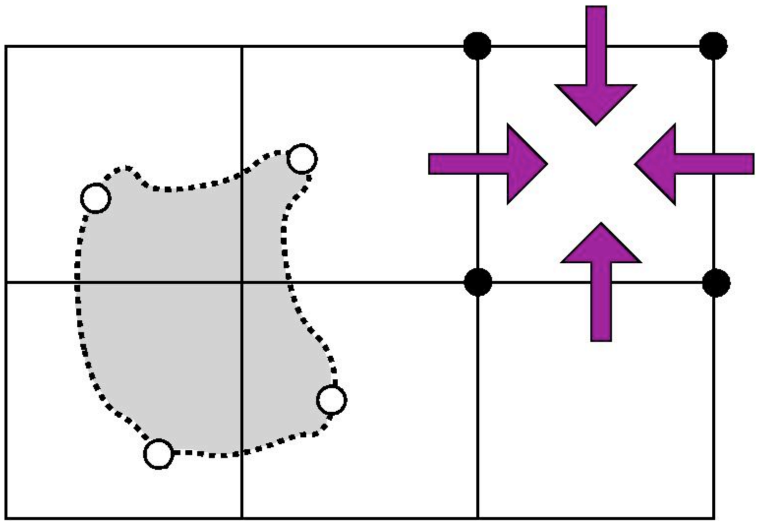

where the angle brackets represent averages in the *x* or *y*-direction and the double-bar refers to the time average over the time-step Δt . So the right-hand side represents the mass transported through each of the four arrival cell faces into the cell during one time step.

$$\overline{\rho}^{n+1}\Delta A = \overline{\rho}^{n}\Delta A - \Delta t \sum_{i=1}^{4} m_i$$

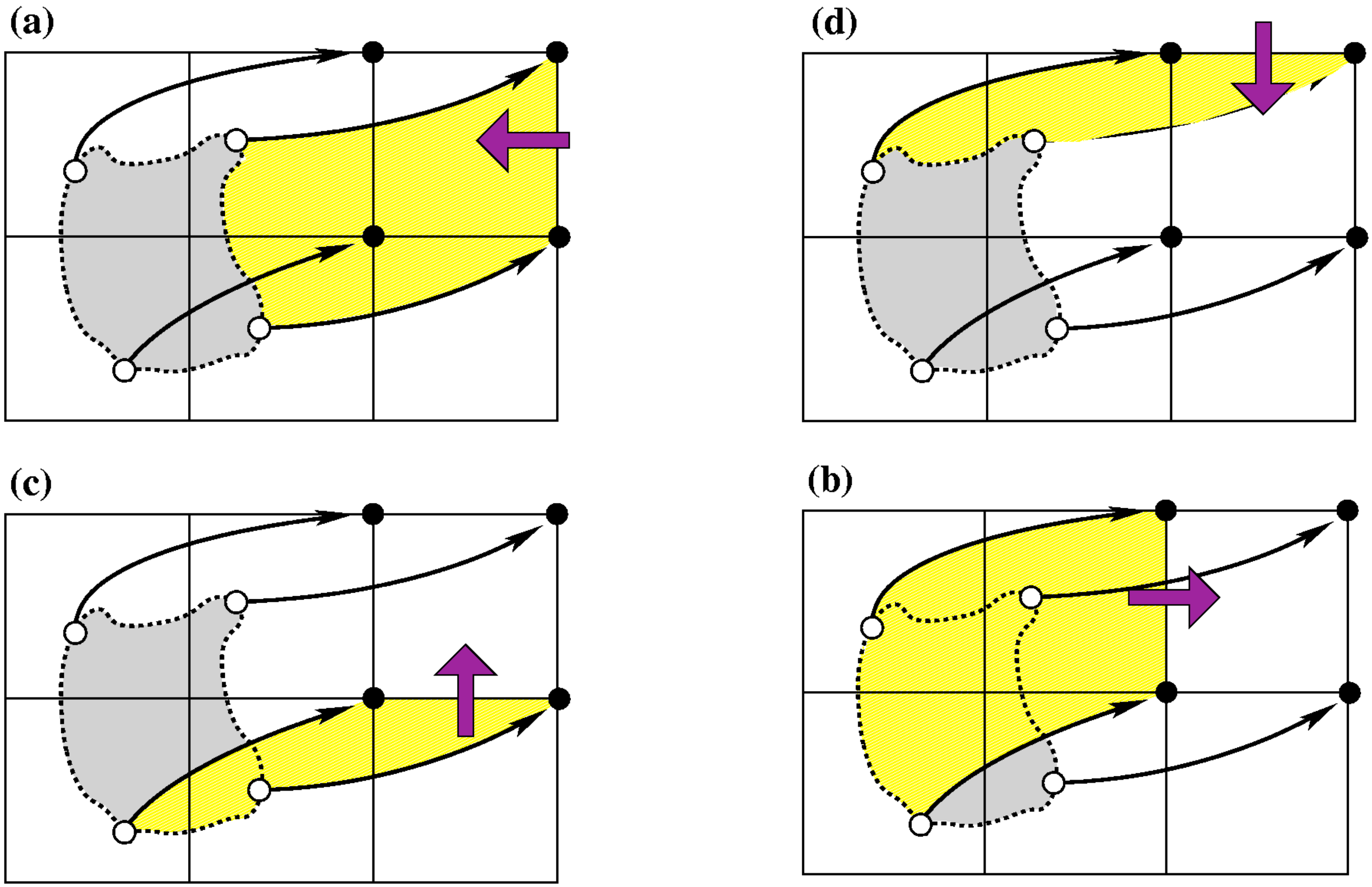

Equivalence between Eulerian and Lagrangian finite-volume schemes

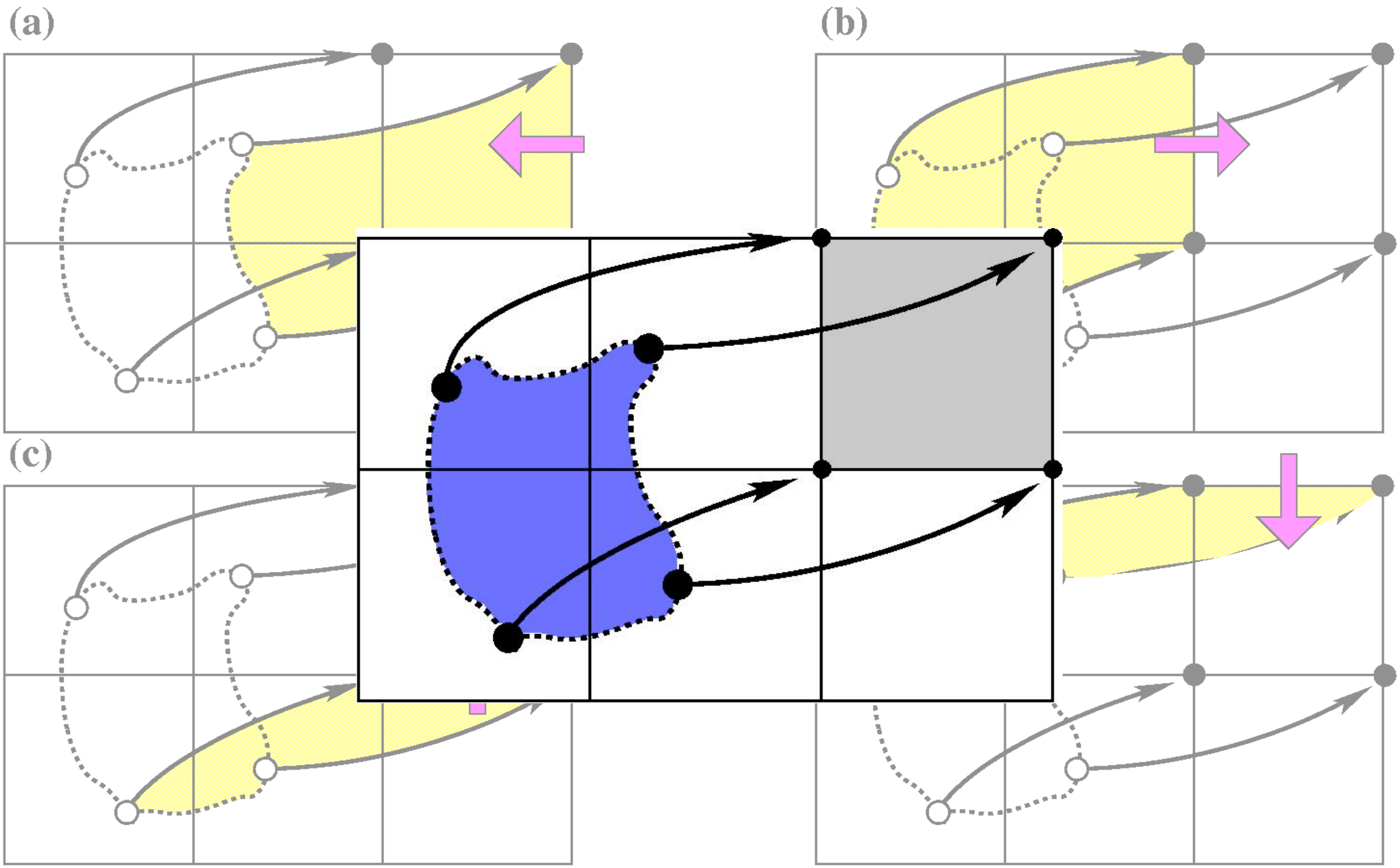

One-dimensional sub-grid-cell reconstruction

Reconstruct the sub-grid-cell distribution in cell i given the adjacent known Eulerian grid cell average values $(\ldots, \overline{\rho}_{i-2}, \overline{\rho}_{i-1}, \overline{\rho}_{i}, \overline{\rho}_{i+1}, \overline{\rho}_{i+2}, \ldots)$ with mass-conservation as a constraint:

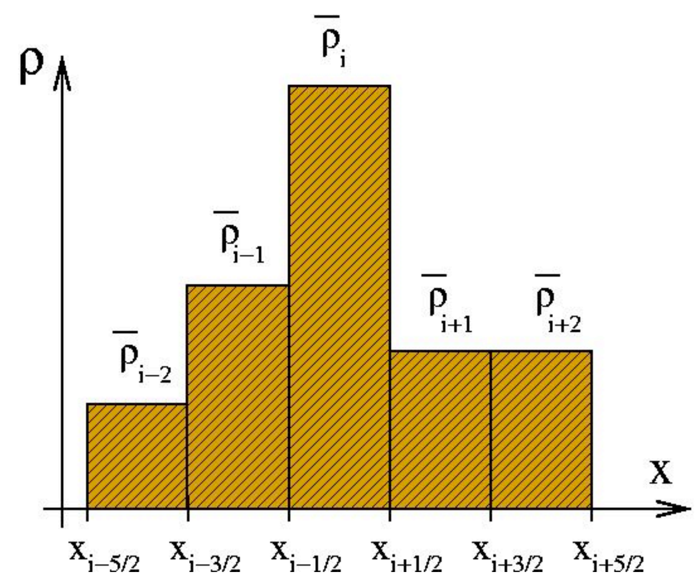

One-dimensional sub-grid-cell reconstruction

Reconstruct the sub-grid-cell distribution in cell *i* given the adjacent known Eulerian grid cell average values $(..., \overline{\rho}_{i-2}, \overline{\rho}_{i-1}, \overline{\rho}_{i}, \overline{\rho}_{i+1}, \overline{\rho}_{i+2}, ...)$ with mass-conservation as a constraint:

Define non-dimensional coordinate $\xi \in [0, 1]$ in the *i*-th cell

$$\xi = \frac{x - x_{i-1/2}}{\Delta x}, \quad x \in [x_{i-1/2}, x_{i+1/2}]$$

• Piecewise Constant Method (PCoM):

$$\rho_i(\xi) = \overline{\rho}_i$$

(Godunov, 1959)

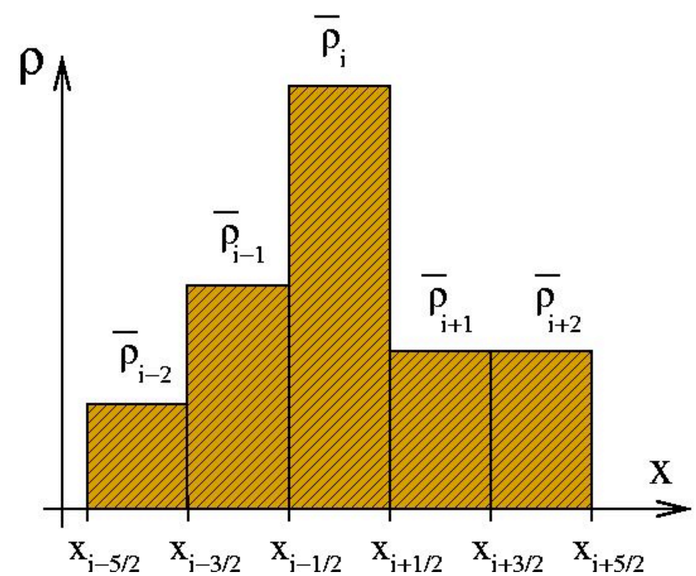

One-dimensional sub-grid-cell reconstruction

Reconstruct the sub-grid-cell distribution in cell *i* given the adjacent known Eulerian grid cell average values $(..., \overline{\rho}_{i-2}, \overline{\rho}_{i-1}, \overline{\rho}_{i}, \overline{\rho}_{i+1}, \overline{\rho}_{i+2}, ...)$ with mass-conservation as a constraint:

Define non-dimensional coordinate $\xi \in [0, 1]$ in the *i*-th cell

$$\xi = \frac{x - x_{i-1/2}}{\Delta x}, \quad x \in [x_{i-1/2}, x_{i+1/2}]$$

• Piecewise Constant Method (PCoM).

• Piecewise Linear Method (PLM):

$$\rho_i(\xi) = \overline{\rho}_i + \frac{1}{2}\left(\overline{\rho}_{i+1} - \overline{\rho}_{i-1}\right)\left(\xi - \frac{1}{2}\right)$$

(Van Leer 1977)

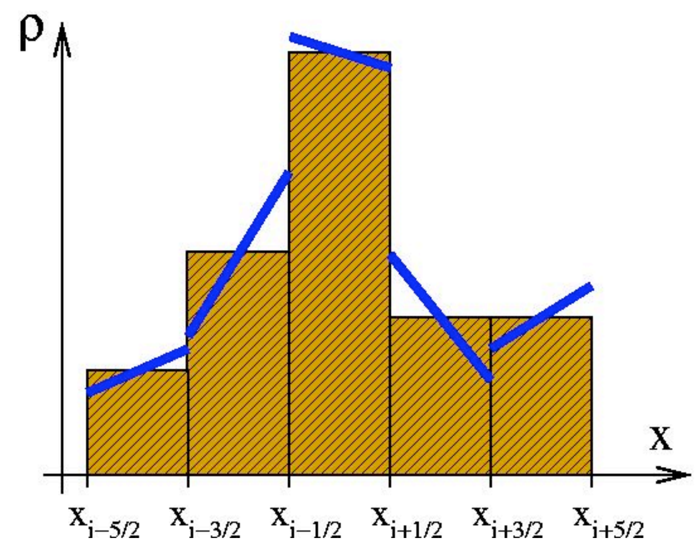

One-dimensional sub-grid-cell reconstruction

Reconstruct the sub-grid-cell distribution in cell i given the adjacent known Eulerian grid cell average values $(..., \overline{\rho}_{i-2}, \overline{\rho}_{i-1}, \overline{\rho}_i, \overline{\rho}_{i+1}, \overline{\rho}_{i+2}, ...)$ with mass-conservation as a constraint:

Define non-dimensional coordinate $\xi \in [0,1]$ in the i-th cell

$$\xi = \frac{x - x_{i-1/2}}{\Delta x}, \quad x \in [x_{i-1/2}, x_{i+1/2}]$$

Polynomials are C^0 at the cell boundaries

- Piecewise Constant Method (PCoM).
- Piecewise Linear Method (PLM).
- Piecewise Parabolic Method (PPM):

$$\rho_i(\xi) = \rho_i^L + \xi \left[\Delta\rho_i + \widetilde{\rho}_i(1-\xi)\right]$$

where $\widetilde{\rho}_i$ and $\Delta\rho_i$ is the "slope" and "curvature" of the polynomial (computed by interpolation). (Collela and Woodward, 1984)

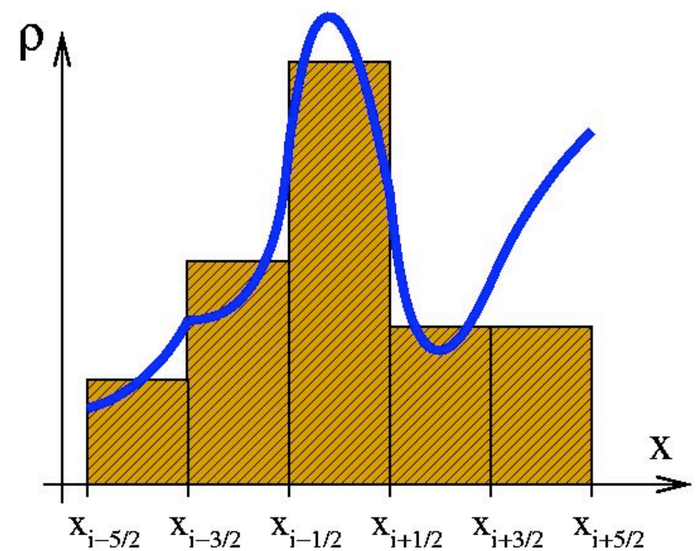

One-dimensional sub-grid-cell reconstruction

Reconstruct the sub-grid-cell distribution in cell i given the adjacent known Eulerian grid cell average values $(\ldots,\overline{\rho}_{i-2},\overline{\rho}_{i-1},\overline{\rho}_{i},\overline{\rho}_{i+1},\overline{\rho}_{i+2},\ldots)$ with mass-conservation as a constraint:

Define non-dimensional coordinate $\xi \in [0,1]$ in the i-th cell

$$\xi = \frac{x - x_{i-1/2}}{\Delta x}, \quad x \in [x_{i-1/2}, x_{i+1/2}]$$

- Piecewise Constant Method (PCoM).
- Piecewise Linear Method (PLM).
- Piecewise Parabolic Method (PPM).
- Piecewise Cubic Method (PCM) and Piecewise Spline Method.

(Zerroukat et al. 2002,4,5,7)

Polynomials are C^0 at the cell boundaries

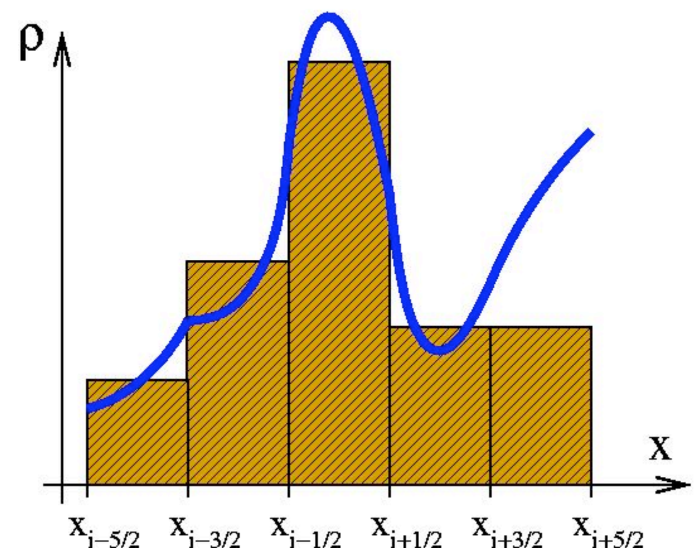

One-dimensional sub-grid-cell reconstruction

Reconstruct the sub-grid-cell distribution in cell i given the adjacent known Eulerian grid cell average values $(\ldots, \overline{\rho}_{i-2}, \overline{\rho}_{i-1}, \overline{\rho}_i, \overline{\rho}_{i+1}, \overline{\rho}_{i+2}, \ldots)$ with mass-conservation as a constraint:

Define non-dimensional coordinate $\xi \in [0,1]$ in the i-th cell

$$\xi = \frac{x - x_{i-1/2}}{\Delta x}, \quad x \in [x_{i-1/2}, x_{i+1/2}]$$

The reconstruction function can be filtered to be rendered positive-definite or monotone.

Polynomials are C^0 at the cell boundaries

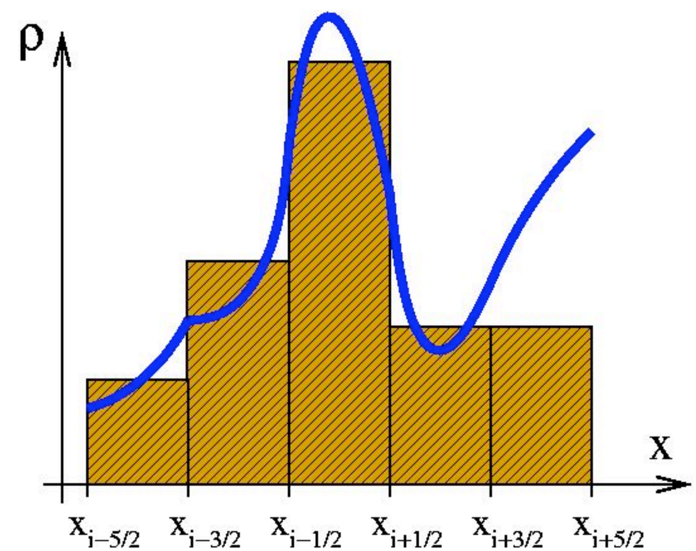

One-dimensional sub-grid-cell reconstruction

Reconstruct the sub-grid-cell distribution in cell i given the adjacent known Eulerian grid cell average values $(\ldots, \overline{\rho}_{i-2}, \overline{\rho}_{i-1}, \overline{\rho}_{i}, \overline{\rho}_{i+1}, \overline{\rho}_{i+2}, \ldots)$ with mass-conservation as a constraint:

Define non-dimensional coordinate $\xi \in [0,1]$ in the i-th cell

$$\xi = \frac{x - x_{i-1/2}}{\Delta x}, \quad x \in [x_{i-1/2}, x_{i+1/2}]$$

The reconstruction function can be filtered to be rendered monotone.

Polynomials no longer guaranteed to be C^0 at the cell boundaries

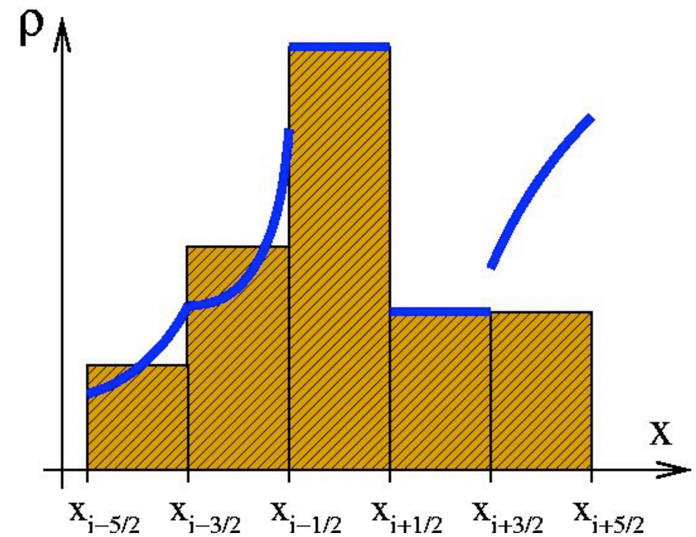

One-dimensional sub-grid-cell reconstruction

Reconstruct the sub-grid-cell distribution in cell *i* given the adjacent known Eulerian grid cell average values $(\ldots,\overline{\rho}_{i-2},\overline{\rho}_{i-1},\overline{\rho}_{i},\overline{\rho}_{i+1},\overline{\rho}_{i+2},\ldots)$ with mass-conservation as a constraint:

Define non-dimensional coordinate $\xi \in [0,1]$ in the *i*-th cell

$$\xi = \frac{x - x_{i-1/2}}{\Delta x}, \quad x \in [x_{i-1/2}, x_{i+1/2}]$$

Polynomials no Longer guaranteed To be C^0 at the cell boundaries

The reconstruction function can be filtered to be rendered monotone.

Less sophisticated filters tend to make the schemes more diffusive than their unlimited versions while dispersion properties can be positively affected by the filter (Durran, 1999).

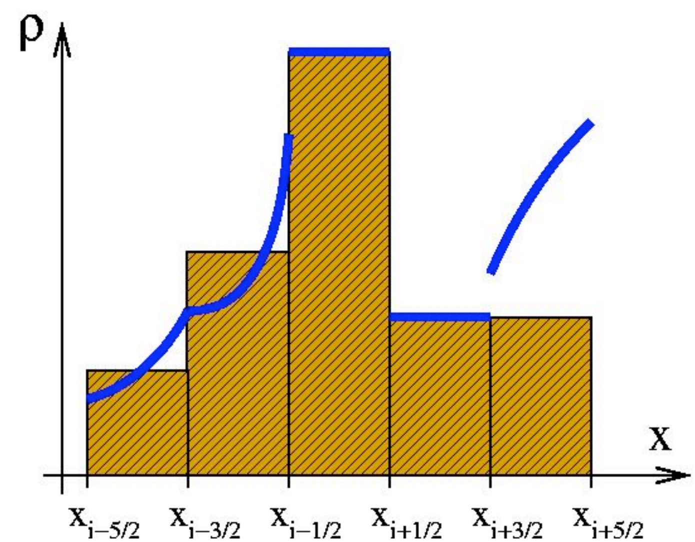

One-dimensional sub-grid-cell reconstruction

Reconstruct the sub-grid-cell distribution in cell *i* given the adjacent known Eulerian grid cell average values $(\ldots, \overline{\rho}_{i-2}, \overline{\rho}_{i-1}, \overline{\rho}_{i}, \overline{\rho}_{i+1}, \overline{\rho}_{i+2}, \ldots)$ with mass-conservation as a constraint:

Define non-dimensional coordinate $\xi \in [0,1]$ in the *i*-th cell

$$\xi = \frac{x - x_{i-1/2}}{\Delta x}, \quad x \in [x_{i-1/2}, x_{i+1/2}]$$

The reconstruction function can be filtered to be rendered monotone.

Less sophisticated filters tend to make the schemes more diffusive than their unlimited versions while dispersion properties can be positively affected by the filters (Durran, 1999).

More advanced filters can even improve overall accuracy of the schemes (Zerroukat et al. 2004).

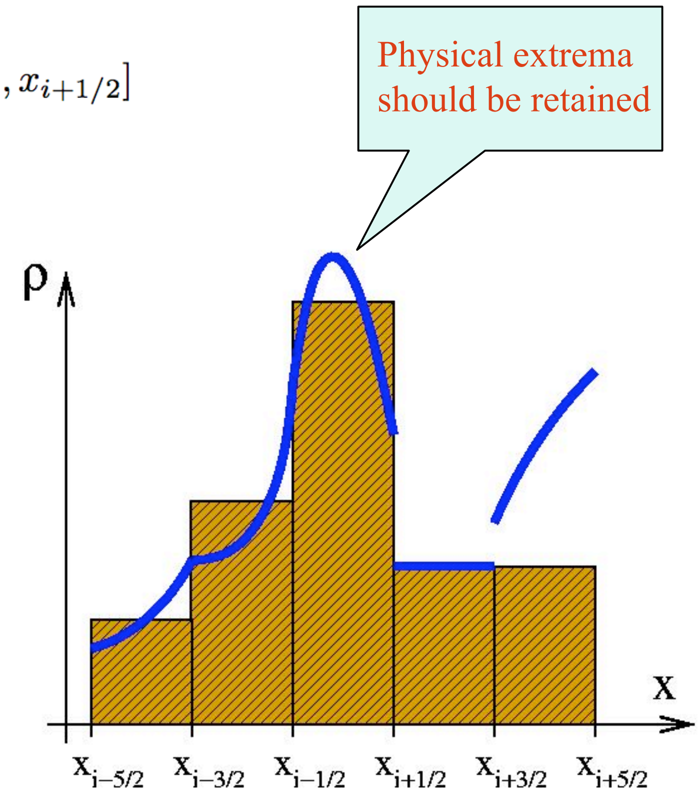

One-dimensional sub-grid-cell reconstruction

Reconstruct the sub-grid-cell distribution in cell i given the adjacent known Eulerian grid cell average values $(\ldots, \overline{\rho}_{i-2}, \overline{\rho}_{i-1}, \overline{\rho}_{i}, \overline{\rho}_{i+1}, \overline{\rho}_{i+2}, \ldots)$ with mass-conservation as a constraint:

Define non-dimensional coordinate $\xi \in [0,1]$ in the i-th cell

$$\xi = \frac{x - x_{i-1/2}}{\Delta x}, \quad x \in [x_{i-1/2}, x_{i+1/2}]$$

The reconstruction function can be filtered to be rendered monotone.

Less sophisticated filters tend to make the schemes more diffusive than their unlimited versions while dispersion properties can be positively affected by the filter (Durran, 1999).

More advanced filters can even improve overall accuracy of the schemes (Zerroukat et al. 2004).

The higher the order of the polynomial the harder it is to limit/filter it

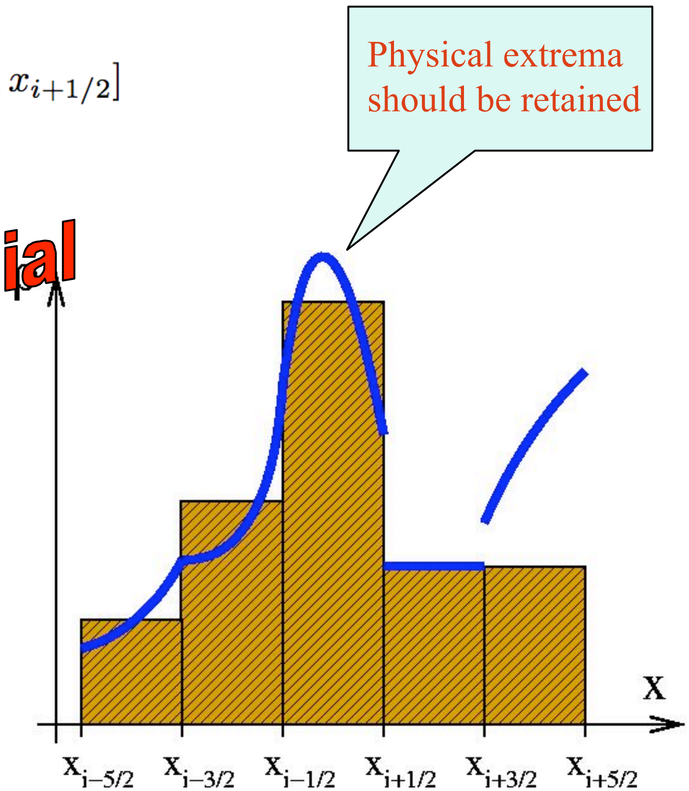

Examples of "higher-order" two-dimensional sub-grid-cell reconstructions

- Fully 2D approach (bi-parabolic):

$$\rho_{ij}(\xi,\eta) = \overline{\rho}^n_{ij} + \rho^W_{ij} + \xi\left[\Delta^\xi \rho_{ij} + \widetilde{\rho}^\xi_{ij}(1-\xi)\right] + \rho^S_{ij} + \eta\left[\Delta^\eta \rho_{ij} + \widetilde{\rho}^\eta_{ij}(1-\eta)\right]$$
$$+c_1\xi\eta + c_2\xi^2\eta + c_3\xi\eta^2 + c_4\xi^2\eta^2$$

Requires the computation of 9 coefficients (Rancic, 1992)

- Quasi 2D approach (quasi-bi-parabolic):

$$\rho_{ij}(\xi,\eta) = \overline{\rho}^n_{ij} + \rho^W_{ij} + \xi\left[\Delta^\xi \rho_{ij} + \widetilde{\rho}^\xi_{ij}(1-\xi)\right] + \rho^S_{ij} + \eta\left[\Delta^\eta \rho_{ij} + \widetilde{\rho}^\eta_{ij}(1-\eta)\right]$$

Neglect "diagonal"/"cross" terms (sum of one-dimensional polynomials)
Nair and Machenhauer (2002)

Examples of "higher-order" two-dimensional sub-grid-cell reconstructions

- Fully 2D approach (bi-parabolic):

$$\rho_{ij}(\xi,\eta) = \overline{\rho}^n_{ij} + \rho^W_{ij} + \xi\left[\Delta^\xi \rho_{ij} + \widetilde{\rho}^\xi_{ij}(1-\xi)\right] + \rho^S_{ij} + \eta\left[\Delta^\eta \rho_{ij} + \widetilde{\rho}^\eta_{ij}(1-\eta)\right]$$
$$+c_1\xi\eta + c_2\xi^2\eta + c_3\xi\eta^2 + c_4\xi^2\eta^2$$

Requires the computation of 9 coefficients (Rancic, 1992)

- Quasi 2D approach (quasi-bi-parabolic):

$$\rho_{ij}(\xi,\eta) = \overline{\rho}^n_{ij} + \rho^W_{ij} + \xi\left[\Delta^\xi \rho_{ij} + \widetilde{\rho}^\xi_{ij}(1-\xi)\right] + \rho^S_{ij} + \eta\left[\Delta^\eta \rho_{ij} + \widetilde{\rho}^\eta_{ij}(1-\eta)\right]$$

Neglect "diagonal"/"cross" terms (sum of one-dimensional polynomials)
(Nair and Machenhauer, 2002)

Note that applying filters in each coordinate direction does not necessarily guarantee monotonicity since the there might be monotonicity violating behavior in the diagonal/cross direction

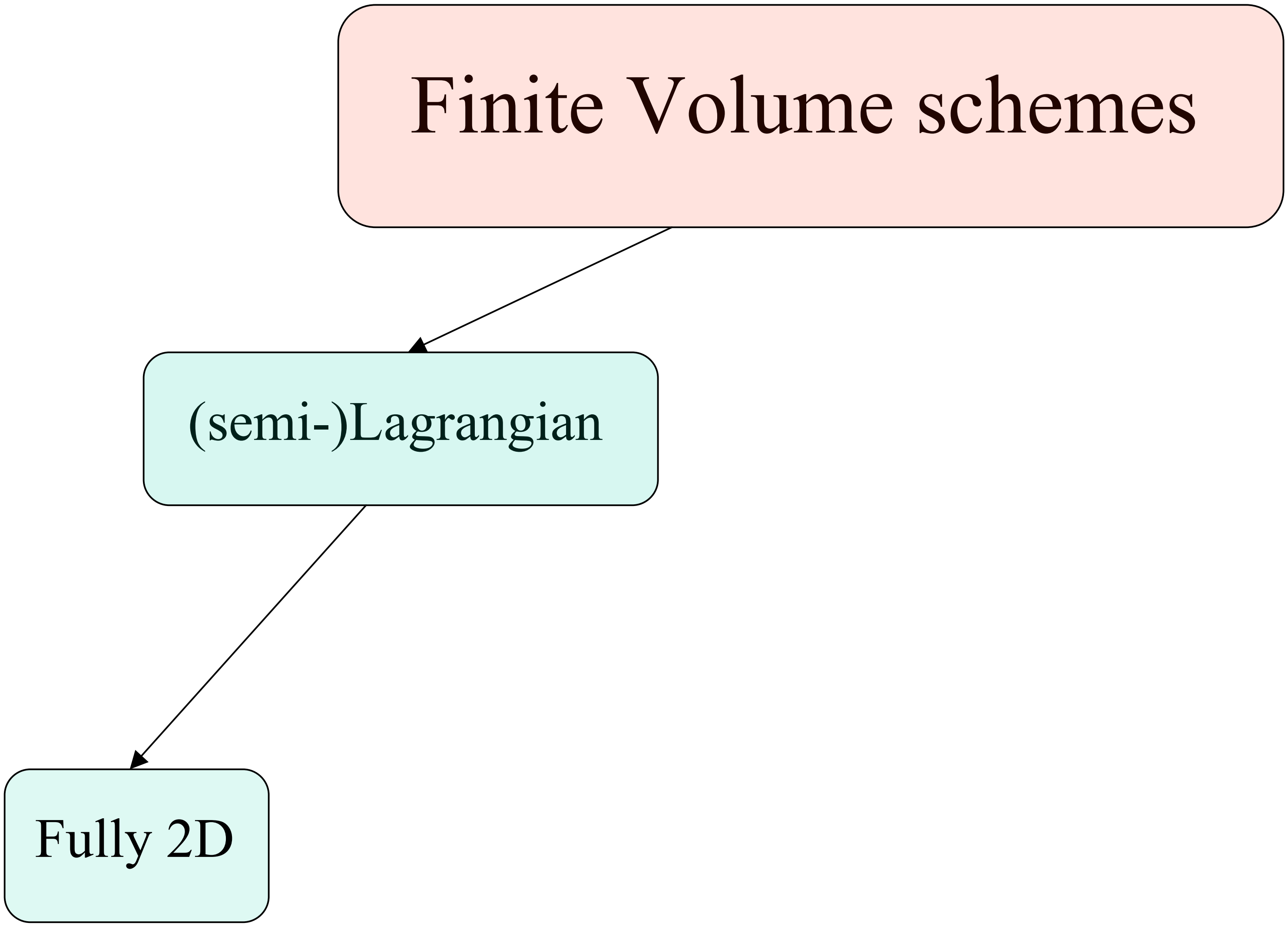
Finite Volume schemes
(semi-)Lagrangian
Fully 2D

Fully two-dimensional CISL scheme

1. Compute upstream trajectories

Solve ODE $\frac{d\vec{r}}{dt} = \vec{v}$ for each cell vertex.

Usually done with an iterative method (see, e.g., Staniforth and Cote, 1990).

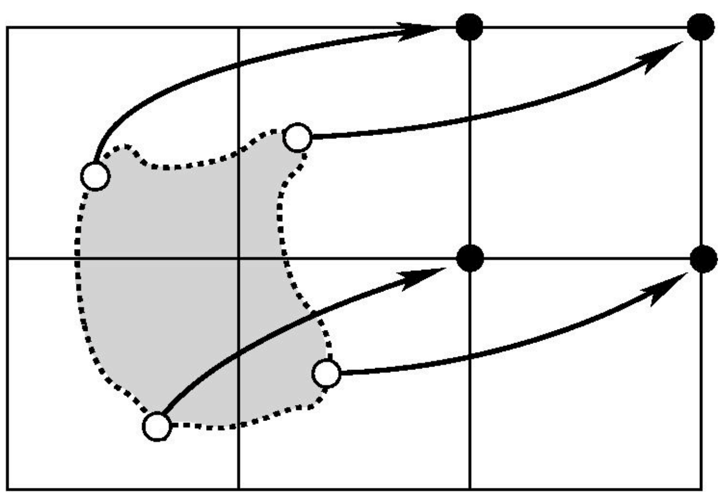

Fully two-dimensional CISL scheme

1. Compute trajectories
2. Approximate departure area

-straight lines (Rancic, 1992): Probably the most accurate approximation to true departure cell, but it is algorithmically more complex to integrate over a general quadrilateral

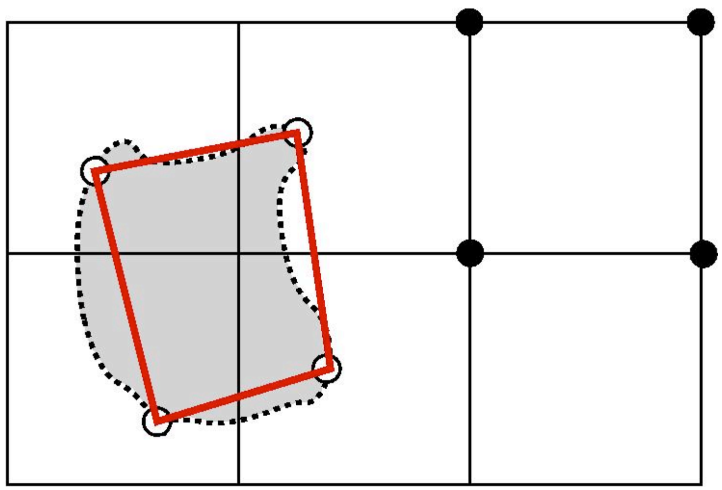

Fully two-dimensional CISL scheme

1. Compute trajectories
2. Approximate departure area

-straight lines (Rancic, 1992): Probably the most accurate approximation to true departure cell, but it is algorithmically more complex to integrate over a general quadrilateral

-lines parallel to coordinate axis (Nair and Machenhauer, 2002): It is algorithmically simpler to integrate over a polygon with sides parallel to the coordinate axis (however, directional bias in cell approximation)

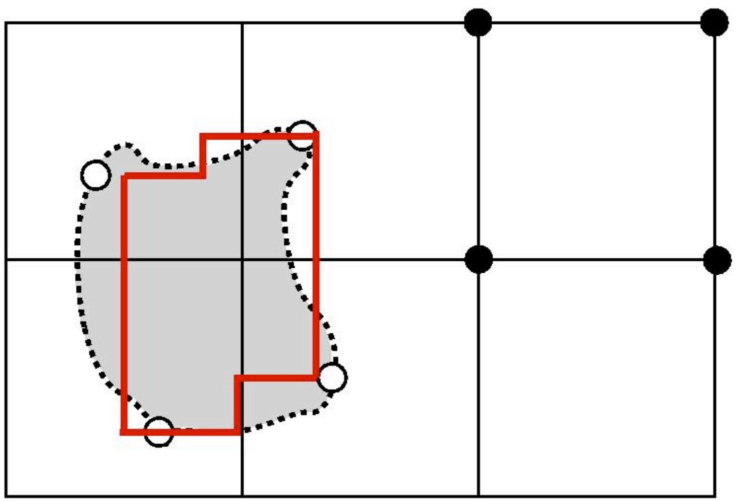

Fully two-dimensional CISL scheme

1. Compute trajectories
2. Approximate departure area
3. Perform sub-grid-cell reconstruction

Approximate $\rho^n(x,y)$ in *ij*-th cell,

$(x,y) \in [x_{i-1/2}, x_{i+1/2}] \times [y_{j-1/2}, y_{j+1/2}]$

from known (Eulerian) cell average values with mass-conservation (and monotonicity) as a constraint.

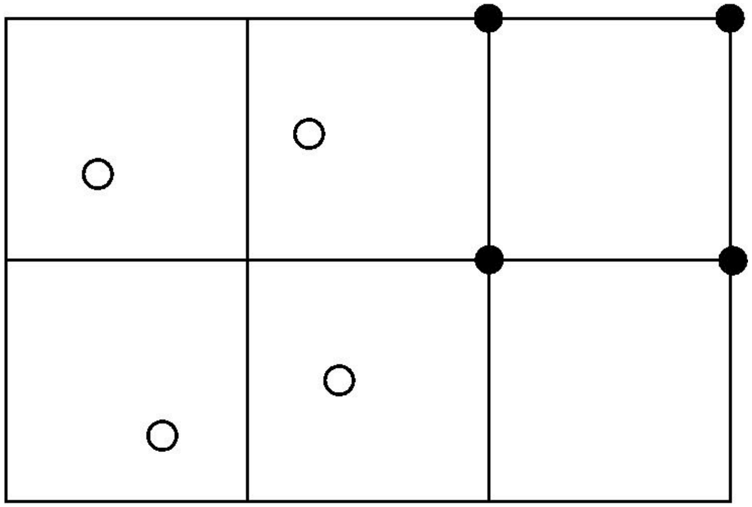

Fully two-dimensional CISL scheme

1. Compute trajectories
2. Approximate departure area
3. Perform sub-grid-cell reconstruction
4. Integrate $\rho^n(x, y)$
   over the departure area

$$\boxed{\overline{\rho}^{n+1}\Delta A = \overline{\rho}^n_* \delta A}$$

$$\overline{\rho}^n_* = \frac{1}{\delta A}\iint_{\delta A} \rho^n(x, y)\, dx\, dy$$

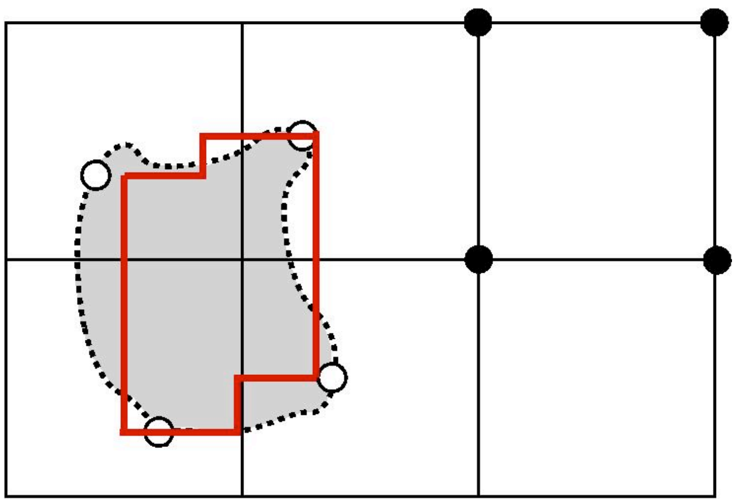

Fully two-dimensional CISL schemes

The global integral of ρ is conserved if the departure cells do not overlap. Mass is conserved locally because we explicitly track mass moving with the flow.

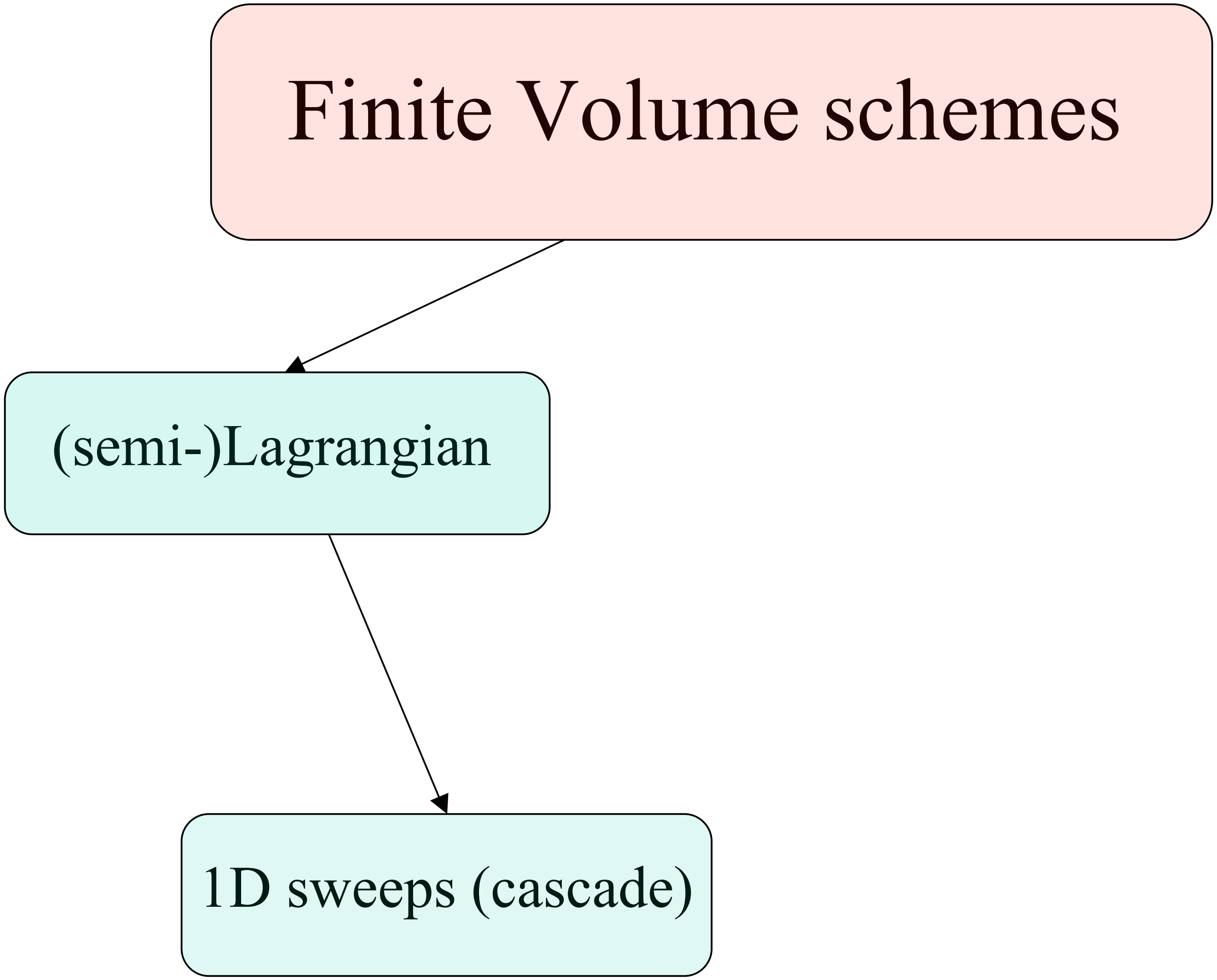
Finite Volume schemes
(semi-)Lagrangian
1D sweeps (cascade)

Cascade CISL scheme

- Cast problem into 1D sweeps (not fixed directional split but flow dependent splitting)

- compute departure points

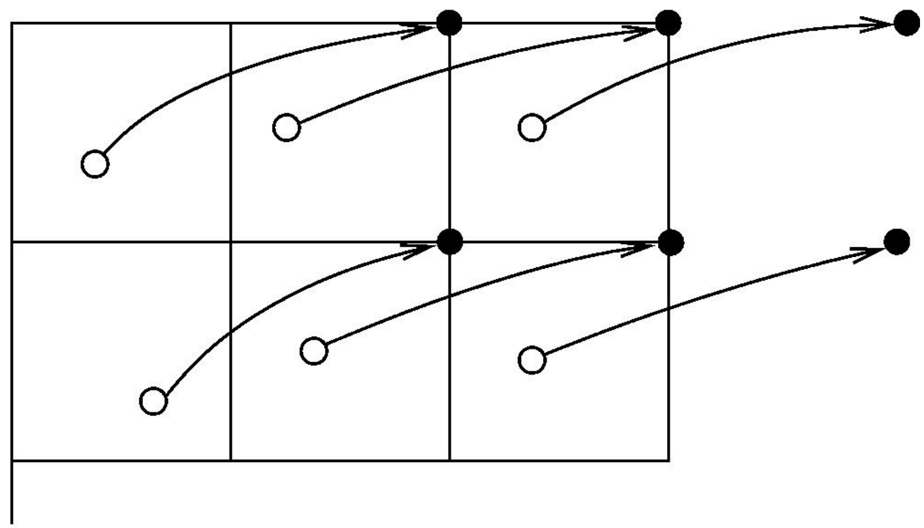

Cascade CISL scheme

- Cast problem into 1D sweeps (not fixed directional split but flow dependent splitting)

- compute departure points
- compute Lagrangian latitudes (fit cubic polynomial along departure points)

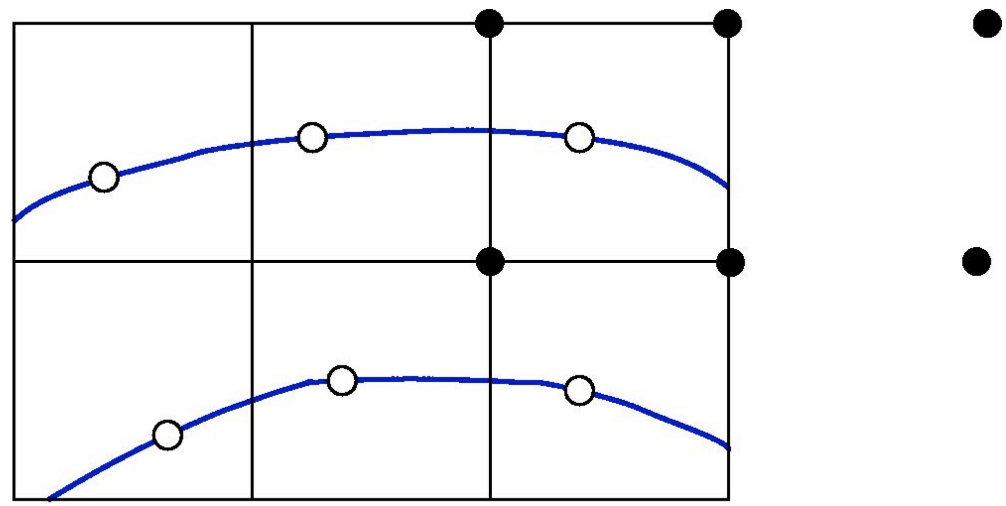

Cascade CISL scheme

- Cast problem into 1D sweeps (not fixed directional split but flow dependent splitting)

- compute departure points
- compute Lagrangian latitudes (fit cubic polynomial along departure points)
- find crossings between Lagrangian latitudes and Eulerian longitudes

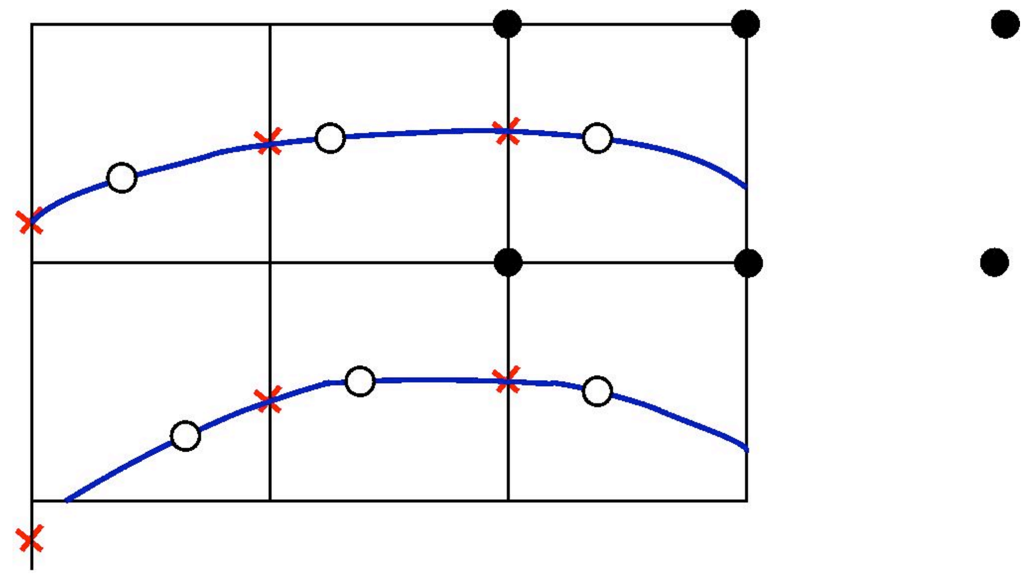

Cascade CISL scheme

- Cast problem into 1D sweeps (not fixed directional split but flow dependent splitting)

- compute departure points
- compute Lagrangian latitudes (fit cubic polynomial along departure points)
- find crossings between Lagrangian latitudes and Eulerian longitudes
- Define upper & lower cell walls
- 1D remap along Eulerian longitudes to intermediate grid

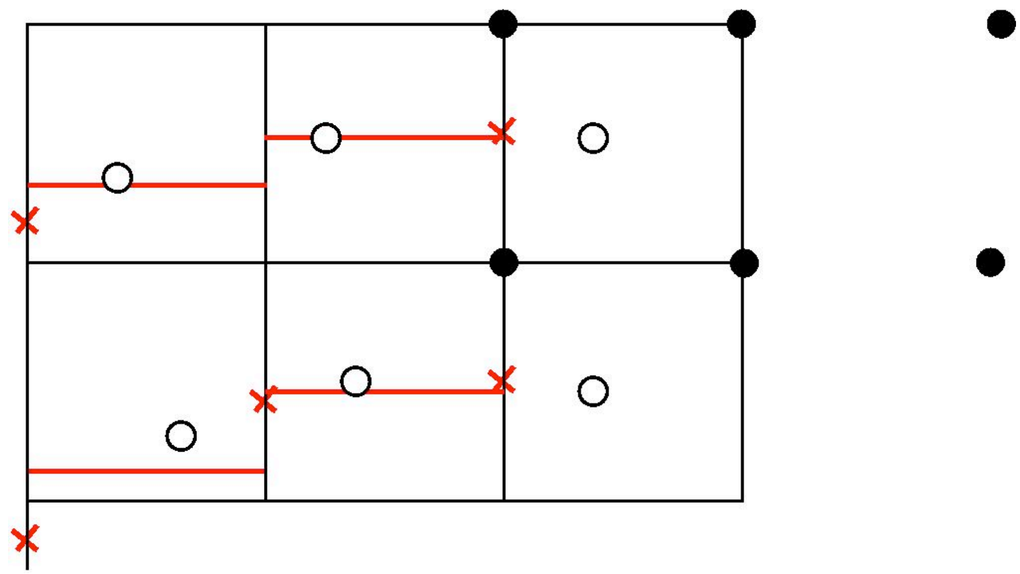

Cascade CISL scheme

- Cast problem into 1D sweeps (not fixed directional split but flow dependent splitting)

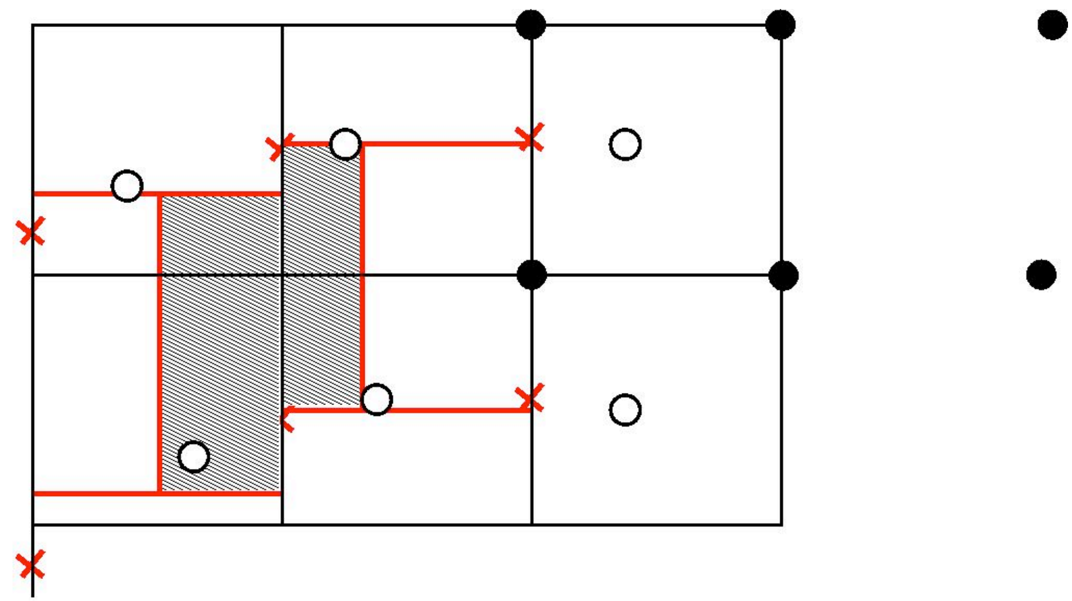

- compute departure points
- compute Lagrangian latitudes (fit cubic polynomial along departure points)
- find crossings between Lagrangian latitudes and Eulerian longitudes
- define upper & lower cell walls
- 1D remap along Eulerian longitudes to intermediate grid
- 1D remap along Lagrangian latitude

Cascade CISL scheme

- Cast problem into 1D sweeps (not fixed directional split but flow dependent splitting)

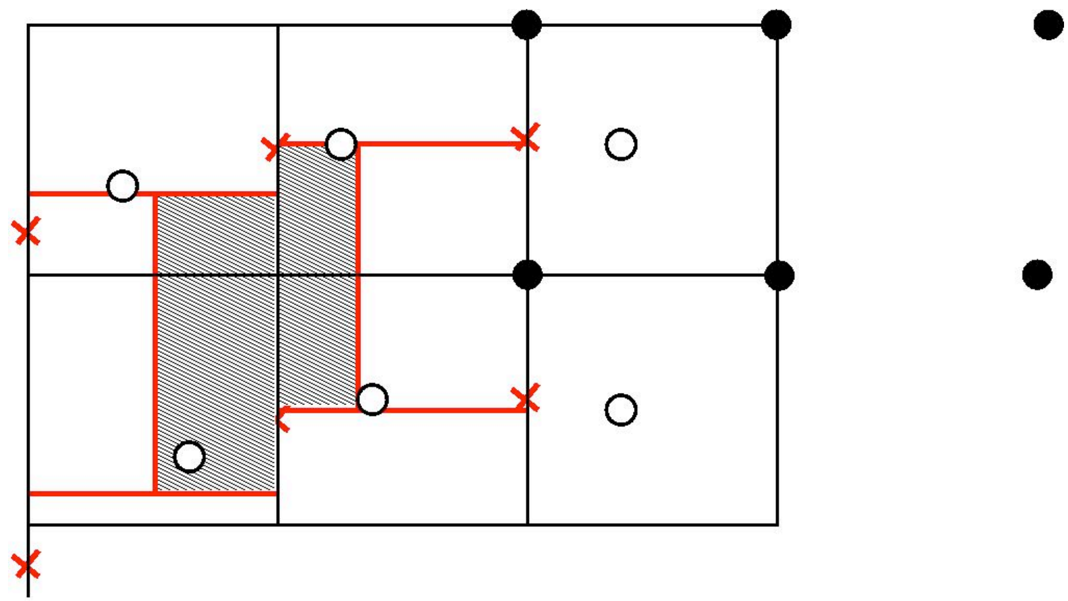

- directional bias (can, however, be alleviated by alternating sweep direction)
- as accurate as 2D CISL scheme of Nair and Machenhauer (2002) in idealized test cases (Nair et al. 2002) as well as in full model runs (Lauritzen et al. 2008)
- filters can be applied with great ease (only need 1D filters)

A note on CISL schemes

- Accuracy of trajectories

  CISL schemes are more sensitive to accurate trajectories than grid-point semi-Lagrangian schemes since the divergence is absorbed in the trajectories (Thuburn 2008, Lauritzen et al. 2005, Kaas 2008):

  Shallow water and hydrostatic tests show that the acceleration should be included in the trajectory estimation when using CISL schemes.
- Since the divergence depends on the trajectories (that are solved for independently), CISL schemes do not (in general) conserve a constant for a non-divergent flow field
- CISL schemes are, however, inherently local and allow for long time steps.

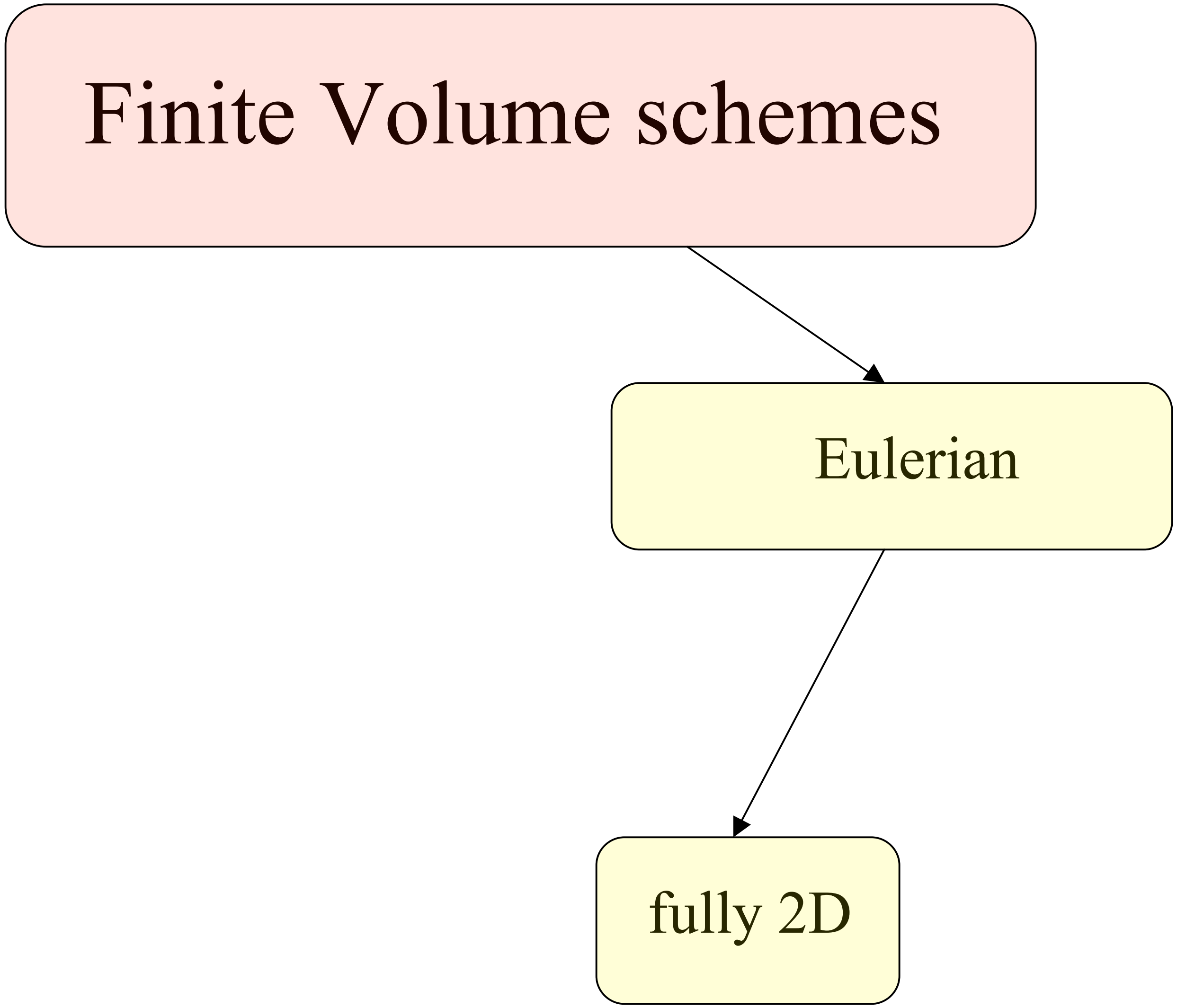
Finite Volume schemes
Eulerian
fully 2D

Finite-volume Eulerian

$$\overline{\rho}^{n+1}\Delta A = \overline{\rho}^{n}\Delta A - \Delta t \sum_{i=1}^{4} m_i$$

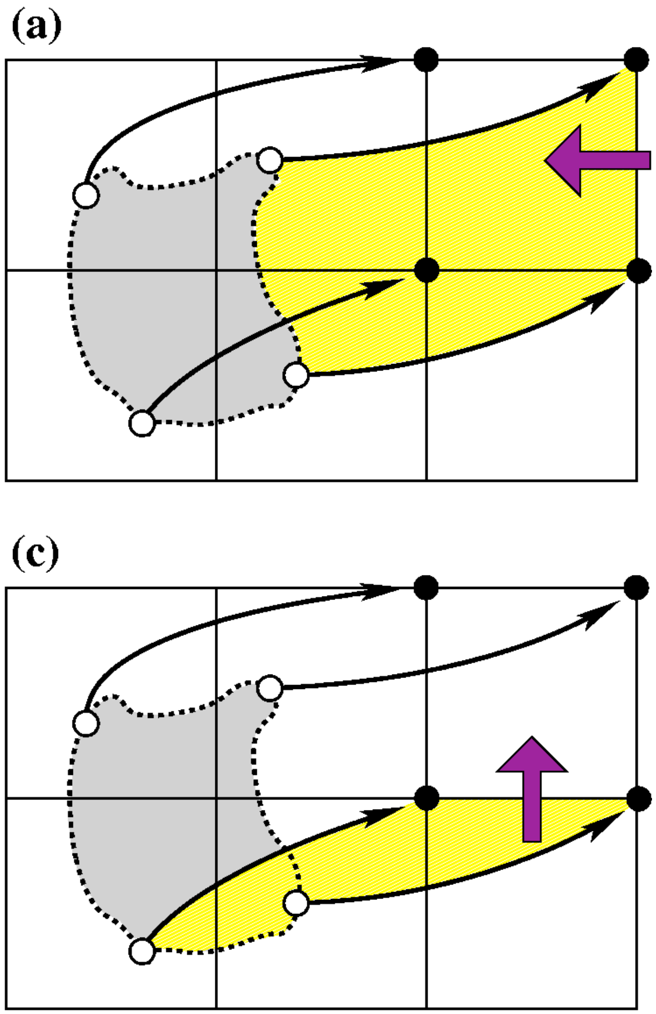

Finite-volume Eulerian

$$\overline{\rho}^{n+1}\Delta A = \overline{\rho}^{n}\Delta A - \Delta t \sum_{i=1}^{4} m_i$$

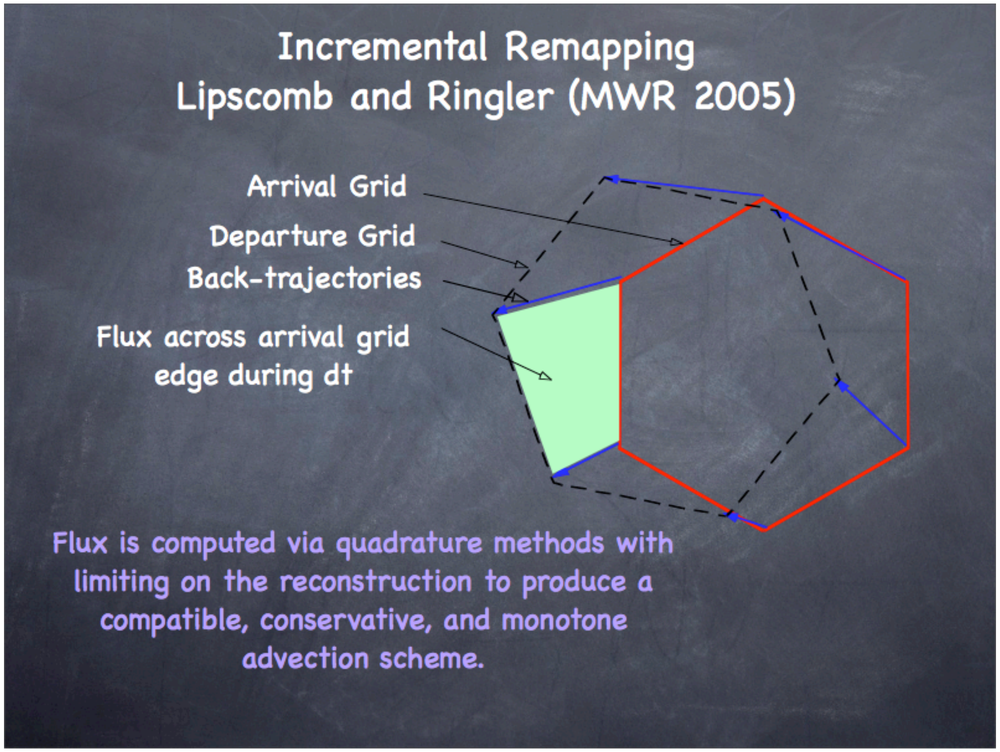

From T.Ringler presentation, NCAR 2008

Approximate trajectories with straight lines …

Usually time-step is limited so that trajectories depart from adjacent cells.

Most Eulerian schemes do not use iterative methods for the trajectories (simply instantaneous winds).

Other Eulerian fully 2D schemes: Smolarkiewicz (1984), Holm (1995) and many more …

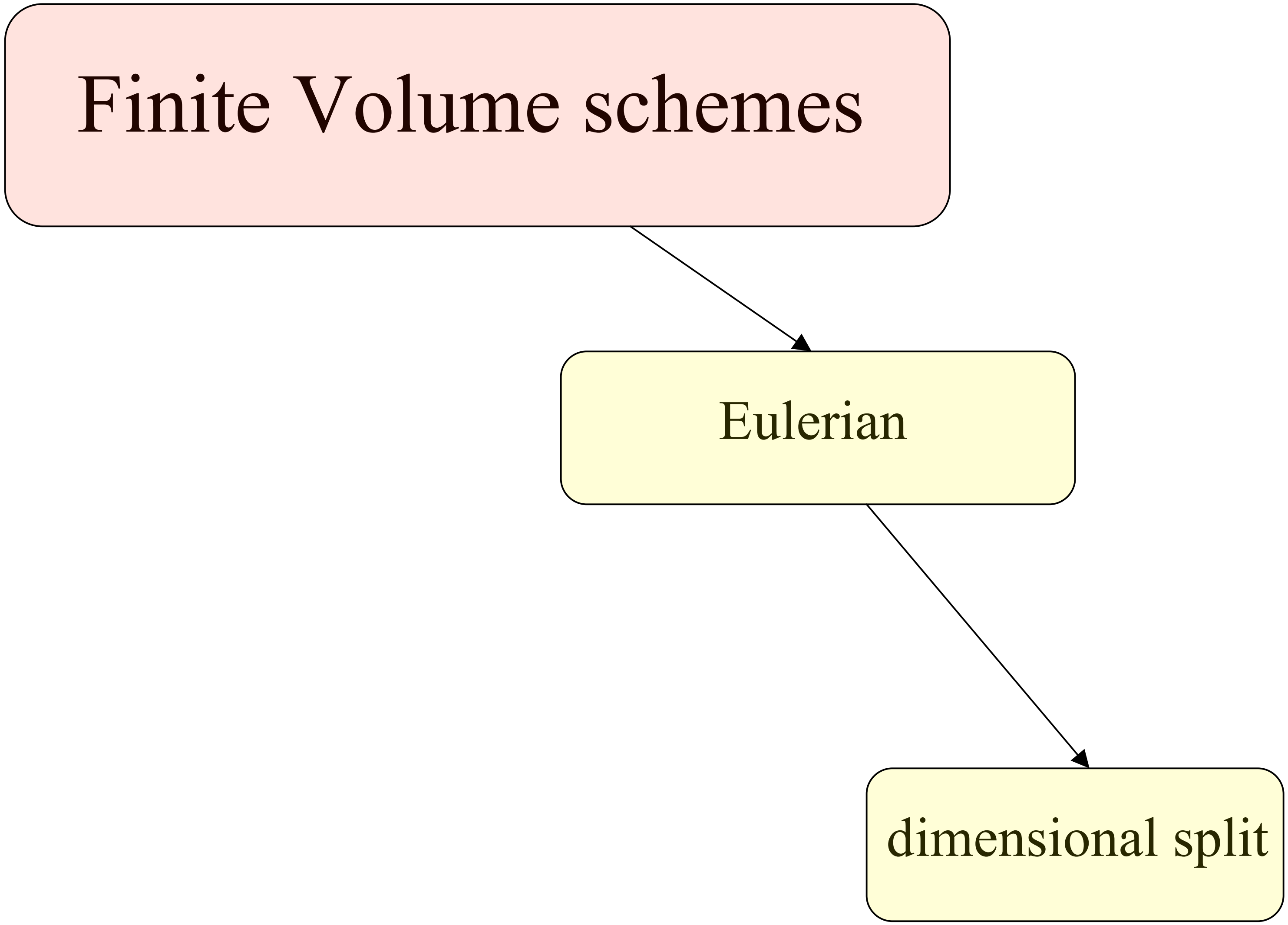

Fixed directional splitting
(not flow dependent splitting)

Finite-volume Eulerian

$$\overline{\rho}^{n+1}\Delta A = \overline{\rho}^{n}\Delta A - \Delta t \sum_{i=1}^{4} m_i$$

Assume a constant traverse wind field

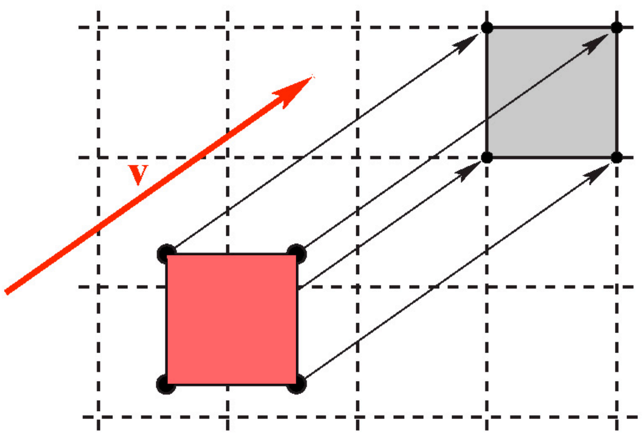

Simple minded operator splitting scheme:

$$\overline{\rho}^{n+1} = \overline{\rho}^{n} + F^{x}\left[\rho\right] + F^{y}\left[\rho\right]$$

where F^x is the flux-divergence in x-direction:

$$F^{x}[\rho] = \frac{1}{\Delta x}\left\{\int_{x_w - u_w^* \Delta t}^{x_w} \rho^n \, dx - \int_{x_e - u_e^* \Delta t}^{x_e} \rho^n \, dx\right\}$$

Finite-volume Eulerian

$$\overline{\rho}^{n+1}\Delta A = \overline{\rho}^{n}\Delta A - \Delta t\sum_{i=1}^{4} m_i$$

Assume a constant traverse wind field

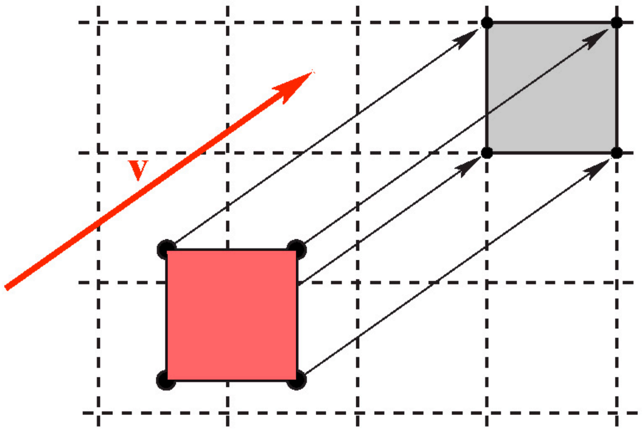

Simple minded operator splitting scheme:

$$\overline{\rho}^{n+1} = \overline{\rho}^{n} + F^{x}\left[\rho\right] + F^{y}\left[\rho\right]$$

where F^{x} is the flux-divergence in x-direction.

Written in "Lagrangian" form (ΔA =1):

Note that

$$F^{x}[\rho] = \iint_{blue} \rho(x,y)\,dx\,dy - \overline{\rho}^{n}$$

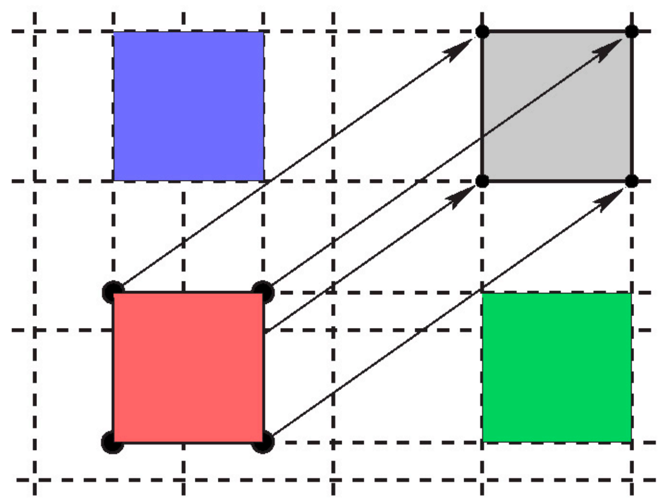

$$\overline{\rho}^{n+1}\Delta A = \overline{\rho}^{n}\Delta A - \Delta t \sum_{i=1}^{4} m_i$$

Assume a constant traverse wind field

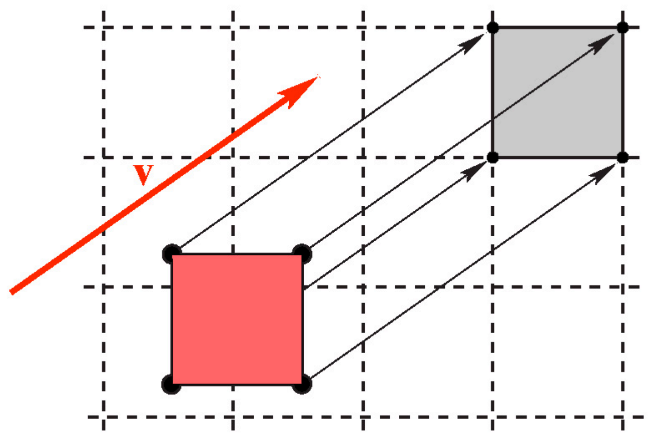

Simple minded operator splitting scheme:

$$\overline{\rho}^{n+1} = \overline{\rho}^{n} + F^{x}\left[\rho\right] + F^{y}\left[\rho\right]$$

where F^{x} is the flux-divergence in x-direction.

Written in "Lagrangian" form (ΔA =1):

$$\overline{\rho}^{n+1} = \iint_{blue} \rho(x,y)dx\,dy + \iint_{green} \rho(x,y)dx\,dy \; - \overline{\rho}^{n}$$

$$\neq \iint_{\delta A} \rho(x,y)dx\,dy$$

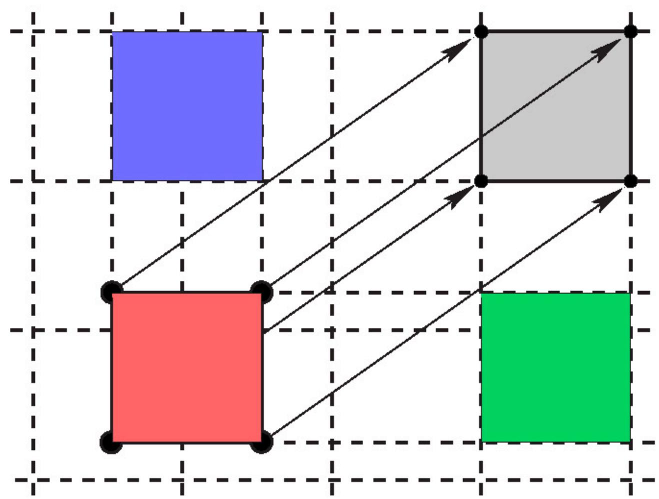

Finite-volume Eulerian

$$\bar{\rho}^{n+1}\Delta A = \bar{\rho}^{n}\Delta A - \Delta t\sum_{i=1}^{4} m_i$$

Assume a constant traverse wind field

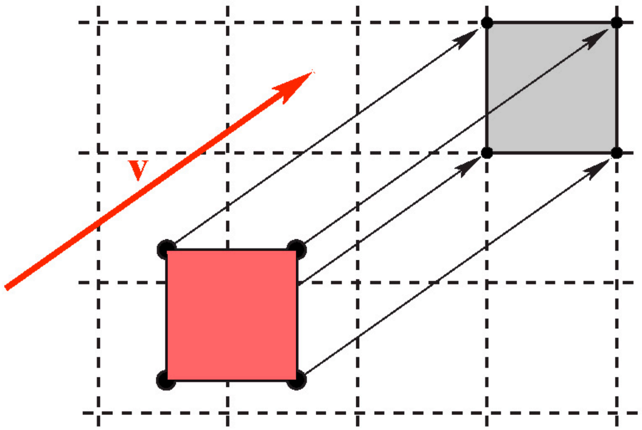

Simple minded operator splitting scheme:

$$\bar{\rho}^{n+1} = \bar{\rho}^{n} + F^x\left[\rho\right] + F^y\left[\rho\right]$$

where F^x is the flux-divergence in x-direction.

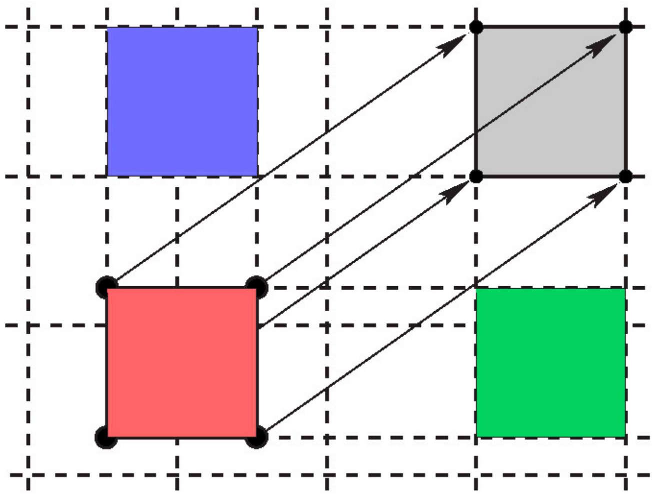

Written in "Lagrangian" form (ΔA =1):

$$\bar{\rho}^{n+1} = \iint_{blue} \rho(x,y)dx\,dy + \iint_{green} \rho(x,y)dx\,dy \; - \bar{\rho}^{n}$$

$$\neq \iint_{\delta A} \rho(x,y)dx\,dy$$

Inconsistent (and unstable) - diagonal flux ignored

Stable if CDF<1 and using first-order operators (Leith, 1965)

Finite-volume Eulerian

$$\bar{\rho}^{n+1}\Delta A = \bar{\rho}^{n}\Delta A - \Delta t \sum_{i=1}^{4} m_i$$

Assume a constant traverse wind field

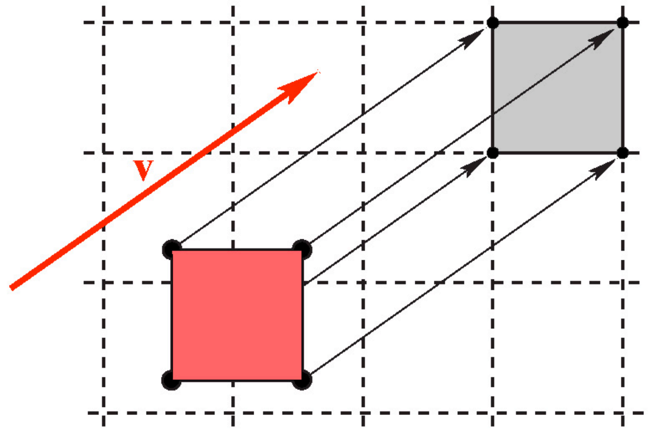

Spatially symmetric scheme:

$$\bar{\rho}^{n+1} = \bar{\rho}^{n} + F^{x}\left[\frac{1}{2}\left(\rho + F^{y}\right)\right] + F^{y}\left[\frac{1}{2}\left(\rho + F^{x}\right)\right]$$

where F^{x} is the flux-divergence in x-direction.

Written in "Lagrangian" form (ΔA=1):

$$\bar{\rho}^{n+1} = \iint_{\delta A} \rho(x,y)\,dx\,dy$$

Consistent for a constant (in space) wind field but for non-divergent but highly deformational flows there is a strong splitting error ($\partial u/\partial x$ evaluated in a different location than $\partial v/\partial y$)

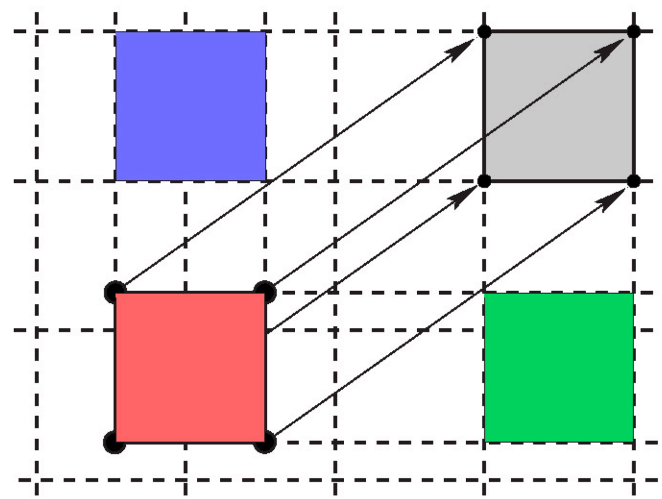

Finite-volume Eulerian

$$\overline{\rho}^{n+1}\Delta A = \overline{\rho}^{n}\Delta A - \Delta t \sum_{i=1}^{4} m_i$$

Assume a constant traverse wind field

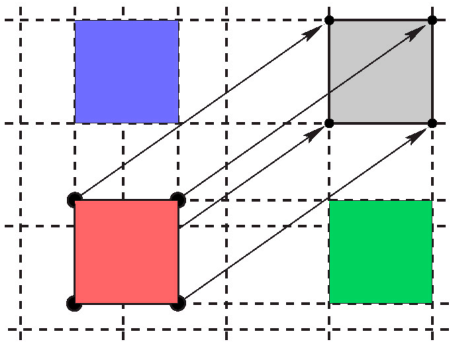

Lin & Rood (1996), Leonard et al. (1996) scheme:

$$\overline{\rho}^{n+1} = \overline{\rho}^{n} + F^x\left[\frac{1}{2}\left(\rho + f^y\right)\right] + F^y\left[\frac{1}{2}\left(\rho + f^x\right)\right]$$

where f^x is the advective operator in x-direction.

No spurious contributions from "divergent part" of inner operators

=> Preserves a constant for a non-divergent wind field

Finite-volume Eulerian

$$\overline{\rho}^{n+1}\Delta A = \overline{\rho}^{n}\Delta A - \Delta t \sum_{i=1}^{4} m_i$$

Assume a constant traverse wind field

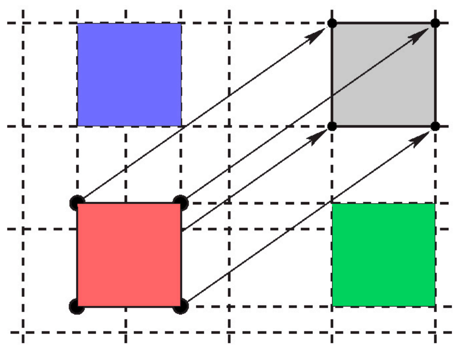

Lin & Rood (1996), Leonard et al. (1996) scheme:

$$\overline{\rho}^{n+1} = \overline{\rho}^{n} + F^x\left[\frac{1}{2}\left(\rho + f^y\right)\right] + F^y\left[\frac{1}{2}\left(\rho + f^x\right)\right]$$

where f^x is the advective operator in x-direction.

Written in "Lagrangian" form (ΔA =1):

$$\overline{\rho}^{n+1} = \iint_{\delta A} \rho(x,y)dx\,dy + \left[I^x - \tilde{I}^x + I^y - \tilde{I}^y\right]$$

where I^x and $\tilde{I}^x$ are the integrals over the blue area associated with flux and advective x-operator, respectively.

These operators must cancel otherwise there is a spurious non-local contribution to the forecast

(Lauritzen 2007)

Von Neuman stability analysis of the Lin & Rood scheme

Amplification factor (for traverse waves $L_x = L_y$ and $u_0 = v_0$)

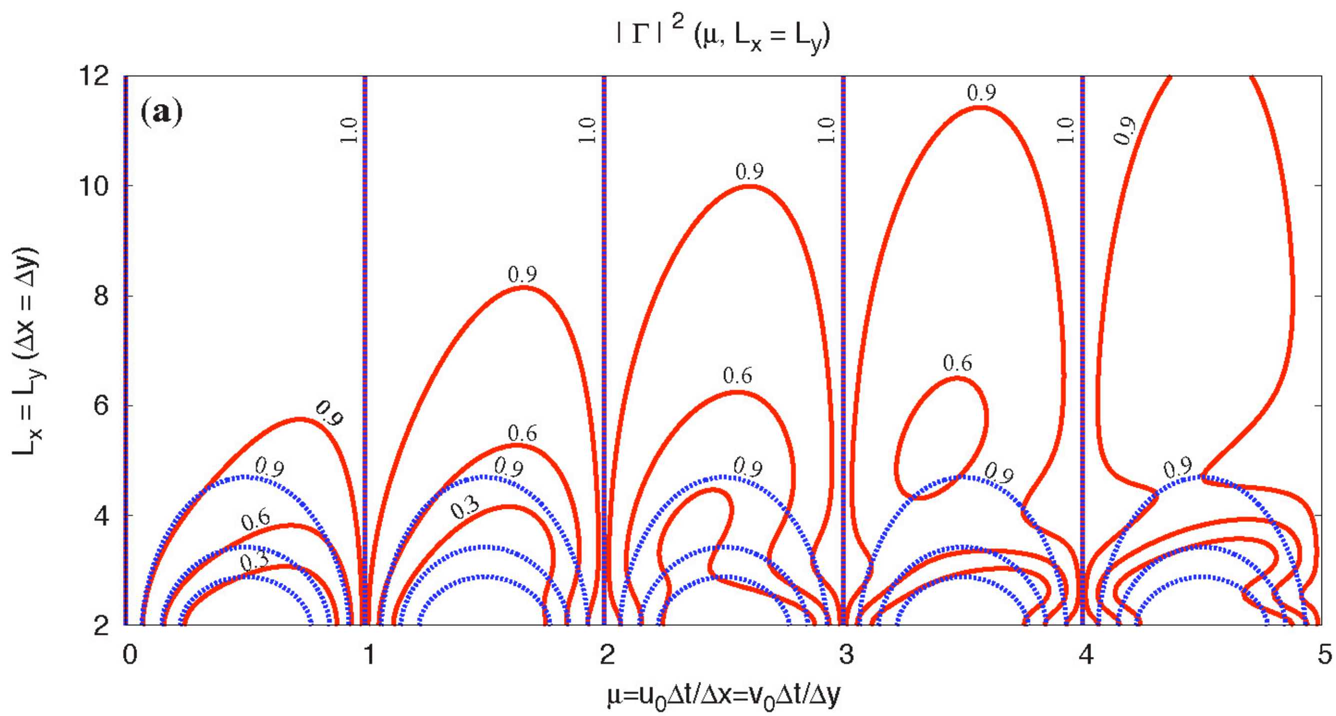

- LR-3-1: I third order (PPM) and $\tilde{I}$ first order (PCM) - FV-CAM
- LR-3-3: I third order (PPM) and $\tilde{I}$ third order (PPM)

(Lauritzen 2007)

Von Neumann stability analysis of the Lin & Rood scheme

Amplification factor (for traverse waves $L_x = L_y$ and $u_0 = v_0$)

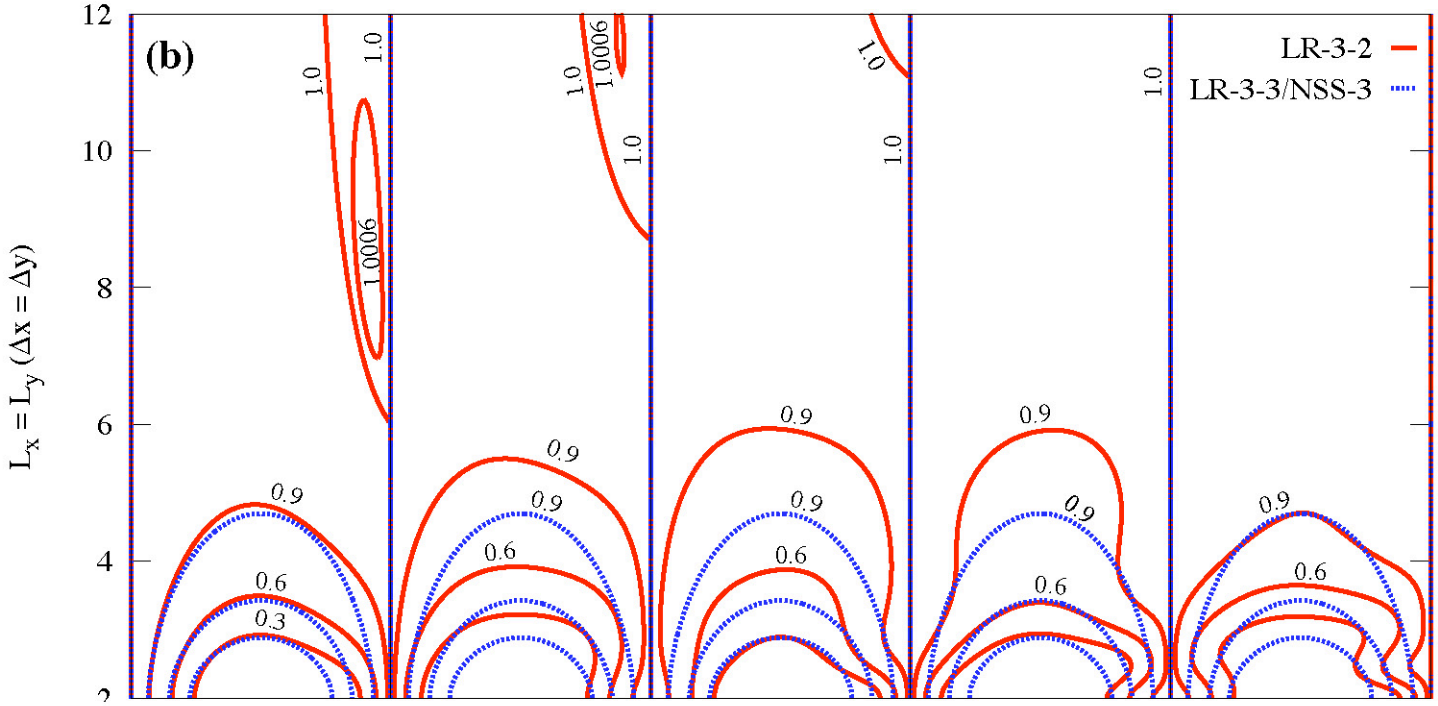

- LR-3-2: I third order (PPM) and $\tilde{I}$ second order (PLM)
- LR-3-3: I third order (PPM) and $\tilde{I}$ third order (PPM)

(Lauritzen 2007)

Von Neumann stability analysis of the Lin & Rood scheme

Dispersion error: Relative frequency (for traverse waves $L_x = L_y$ and $u_0 = v_0$)

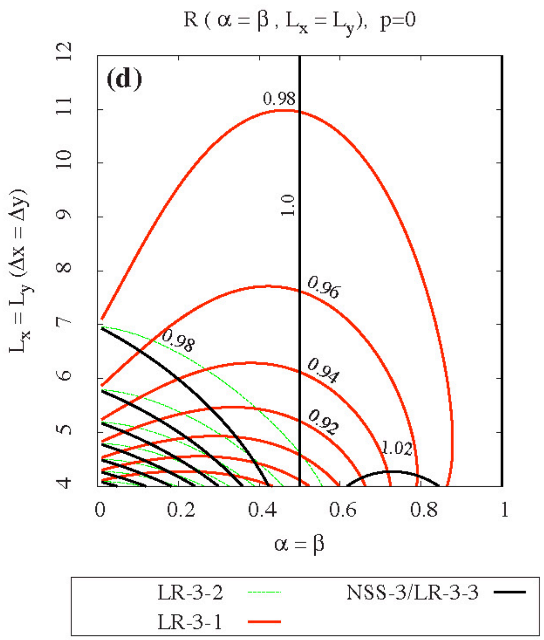

$$R = \frac{\text{numerical frequency}}{\text{analytical frequency}}$$

- Non-local contributions to forecast significantly increase dispersion errors!

(Lauritzen 2007)

Finite-volume Eulerian

$$\overline{\rho}^{n+1}\Delta A = \overline{\rho}^{n}\Delta A - \Delta t \sum_{i=1}^{4} m_i$$

Lin & Rood (1996), Leonard et al. (1996) scheme:

$$\overline{\rho}^{n+1} = \overline{\rho}^{n} + F^x\left[\frac{1}{2}(\rho + f^y)\right] + F^y\left[\frac{1}{2}(\rho + f^x)\right]$$

where f^x is the advective operator in x-direction.

Assume we use the same inner and outer operators (no spurious contributions from non-local areas for constant, in space and time, flows). What does the effective departure area look like for a rotational and divergent flow (example):

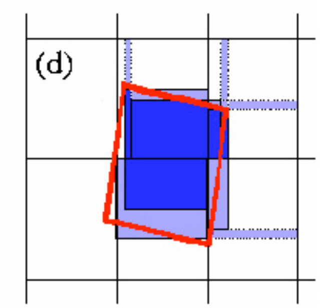

Still some small but non-local contributions to the forecast

(Machenhauer et al. 2008)

Filters: *A Priori* & *A Posteriori*

- *A priori*: Filters introduced before the estimation of fluxes or upstream cell integrations (already discussed)
- *A posteriori*: Flux limiters, e.g., FCT (Flux Corrected Transport) introduced by Boris and Book (1976) and Zalesak (1979). Basic idea:

  Combine higher-order fluxes (which are accurate but not monotone) and low-order fluxes (which are diffusive but monotone).

  "Nudge" the low-order flux as much towards the high-order fluxes without violating monotonicity constraints.

Several types of flux limiters: Bott (1989), Smolarkiewicz and Grabowski (1990), Rasch (1994), Holm (1995), Xue (2000), etc.

Questions 

References

All references can be found in

Bennert Machenhauer, Eigil Kaas and Peter H. Lauritzen. 2008:
Finite-Volume Methods in Meteorology. Chapter in *Handbook of Numerical Analysis: Special Volume on Computational Methods for the Atmosphere and the Oceans*: 120 pp.

see http://www.cgd.ucar.edu/cms/pel/publications.html